ABSTRACT

$BRAF^{V600E}$ is the most common mutation in papillary thyroid carcinoma (PTC). Tissue inhibitor of metalloproteinases (TIMP-1) and Nuclear Factor (NF)-κB have been shown to play an important role in thyroid cancer. Our aim was to evaluate whether an interplay among these three factors exerts a functional role in PTCs. 56 PTC specimens were analyzed for $BRAF^{V600E}$ mutation, TIMP-1 expression and NF-κB activation by real-time allele-specific amplification, real-time quantitative PCR (qRT-PCR) and electroforetic mobility shift assay (EMSA), respectively. We show that $BRAF^{V600E}$ mutation occurs selectively in PTC nodules and determines up-regulation of TIMP-1 and hyperactivation of NF-κB. In addition we describe that CD63, a member of the tetraspanin family, which has been indicated as the TIMP-1 receptor, was selectively up-regulated in PTC nodules harboring $BRAF^{V600E}$ mutation.

The proof of the principle was assayed *in vitro* using BCPAP cell line harboring $BRAF^{V600E}$ mutation. When we silenced *BRAF* gene in BCPAP cell line using a specific small interfering RNA for the mutated form (MU-A), we found a marked decrease in *TIMP-1* expression and NF-κB binding activity. Furthermore, using invasion assay we found that MU-A treated cells decreased significantly their ability to invade. We demonstrate that $BRAF^{V600E}$ causes up-regulation of TIMP-1 via NF-κB activation. TIMP-1 binds its surface receptor CD63, leading to Akt activation, and thus conferring an anti-apoptotic behavior which eventually promotes cell invasion. We individuated a functional trilogy which might explain how $BRAF^{V600E}$ determines cancer initiation, progression and invasiveness in PTC.

INTRODUCTION

CHAPTER 1: THYROID CANCER

The unique and fundamental function of the follicular epithelial thyroid cells is to utilize iodide as a substrate to synthesize thyroid hormones to meet the normal metabolism of the body, a process that involves several thyroid-specific iodide-handling protein molecules (1). In this process, iodide is transported from the blood stream into the thyroid cell through the sodium/iodide symporter (NIS) in the basal membrane, followed by its transportation into the follicular lumen through such transporters as pendrin (also called SLC26A4) in the apical membrane of the cell. Through thyroid peroxidase (TPO), iodide is oxidized and organified into thyroglobulin (Tg) through iodination of tyrosine residues in Tg for the formation of thyroid hormones. The thyroid-specific transcription factors TTF-1, TTF-2, and Pax-8 play an important role in the regulation of these thyroid genes. The entire process is up-regulated by the thyroid-stimulating hormone (TSH) that acts by binding to the TSH receptor (TSHR) on the cell membrane (2).

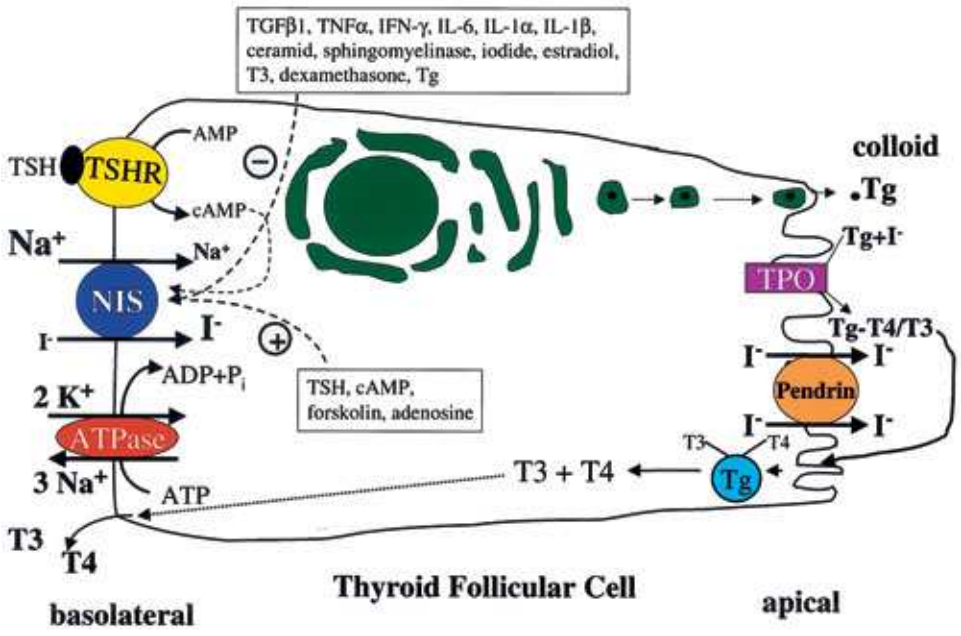

Graphic representation of follicular epithelial thyroid cells function.

Thyroid cancer is the most common endocrine malignancy and its incidence is rapidly rising in recent years in the world (3). It accounts for less than 1% of all new malignancies, although occult carcinomas can be found in 5-36% of autoptic studies (4).

In the United States, the rise in the incidence of thyroid cancer is the fastest among cancers in many patient populations, particularly women and elder patients of both genders, with an estimated 2008 incidence of 37,340 cases and a prevalence of above 350,000 cases (5).

Sicily, probably for its geographic characteristics, like to be an island, to have volcanic areas and to have endemic goiter areas, is a geographic area with a very high thyroid cancer incidence, as reported in Thyroid Tumor Sicily Register showed. From January 1 2002 through December 31 2004 this register showed that 1950 patients were newly diagnosed with thyroid cancer (622 in 2002, 677 in 2003, and 651 in 2004). For this period, the ratio of women to men was 4.3 to 1.0. Among both women and men, the age group of 40 – 60 years had the highest incidence of thyroid cancer. The crude annual incidence was 21.9 diagnoses per 100.000 residents per year at risk among women with an age-standardized incidence rate for the world population (ASR_w) of 17.8 diagnoses per 100.000 residents per year; among men, crude annual incidence was 4.7 diagnoses per 100.000 residents per year at risk with an ASR_w of 3.7 diagnoses per 100.000 residents per year (6). Pellegriti et al. also found that 57.7% of all thyroid tumors in Sicily were microcarcinomas (maximum diameter $\leq$10 mm) and that papillary thyroid cancer was the histotype more diagnosed (89.2%).

The major histological types of follicular cell-derived thyroid cancer are papillary thyroid cancer (PTC), follicular thyroid cancer (FTC), and anaplastic thyroid cancer (ATC) (7, 8) which account for approximately 80, 15 and 2% of all

thyroid malignancies, respectively. Benign thyroid adenoma (BTA) is a common endocrine tumor. Medullary thyroid cancer derived from para-follicular cells is a relatively rare malignancy and will not be discussed here.

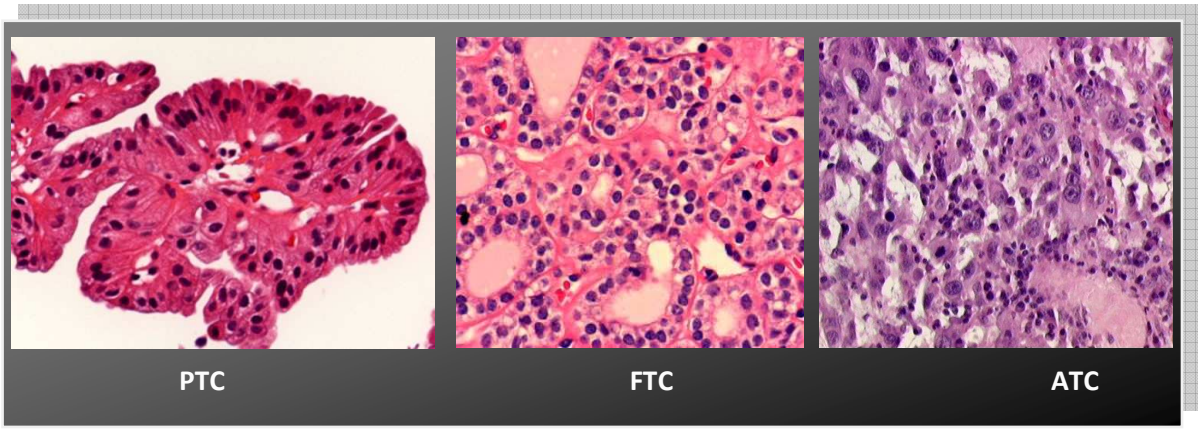

Immunohistochemistries of the major histological types of follicular cell-derived thyroid cancer.

PTC and FTC are generally differentiated, indolent, and highly curable with current treatments. ATC is an undifferentiated and rapidly lethal thyroid cancer (9). In fact, ATC is among the most aggressive and deadly human cancers. There are also poorly differentiated thyroid cancers that have a high incurability and mortality albeit with a better prognosis than ATC. Poorly differentiated thyroid cancer can progress into ATC, and both can derive from PTC and FTC or occur *de novo*.

Thyroid cancers, particularly poorly differentiated thyroid cancer and ATC, can loose the ability to take up iodide and consequently do not respond to radioiodine treatment; they become incurable if they are also surgically inoperable. This is currently a major therapeutic challenge for thyroid cancer and is the main cause of thyroid cancer-related morbidity and mortality (2).

The biological behavior of PTC varies widely, from indolent microcarcinomas, growing slowly with little or no invasion, to invasive tumors that metastasize and cause death. Nevertheless, the small size of the tumor is not necessarily related

to lower malignant potential, as about 10% of PTC patients die from distant metastases, which may appear several years after diagnosis (10, 11).

CHAPTER 2: MAP KINASE SIGNALING PATHWAY AND BRAF MUTATION

The etiology of PTC has not been fully established. The RET/PTC-RAS-BRAF-MEK-ERK pathway (Mitogen-Activated Protein Kinase pathway or MAPK) is a classical conserved intracellular signaling pathway that plays a fundamental role in cell proliferation, differentiation, apoptosis, and survival and, when aberrantly activated, tumorigenesis (12).

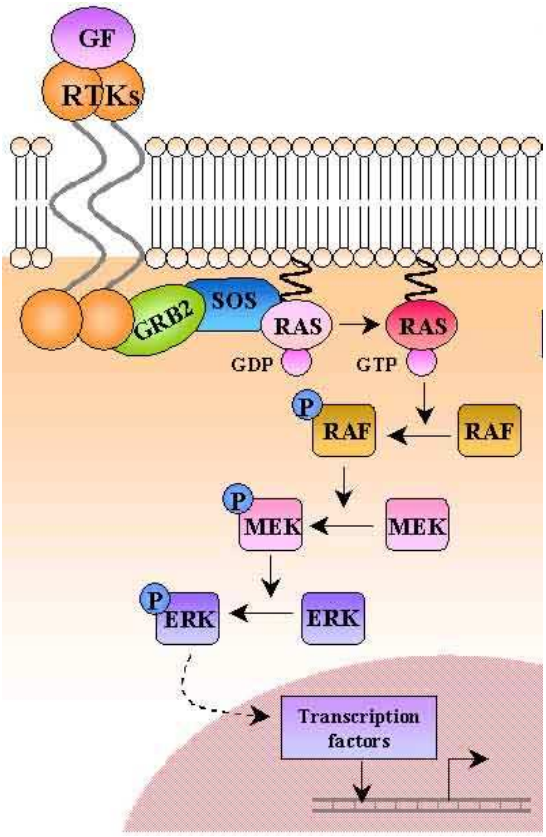

Graphic representation of The RET/PTC-RAS-BRAF-MEK-ERK pathway (Mitogen-Activated Protein Kinase pathway or MAPK).

The classical oncogenic genetic alterations commonly seen in thyroid cancer include Ras mutations (13), RET/PTC rearrangements (14), and PAX8-peroxisome proliferator-activated receptor γ (PPARγ) fusion oncogene (15).

BRAF mutation is a major cause of aberrant activation of the MAP kinase pathway in human cancers (16). Among the three known Raf kinases, A-Raf, B-Raf (BRAF), and C-Raf, BRAF is the most potent activator of the MAP kinase pathway (17).

The discovery of activating mutations of the gene for BRAF has expanded the array of the known genetic alterations that activate the MAP kinase pathway and underscores the importance of this pathway in human cancer (16).

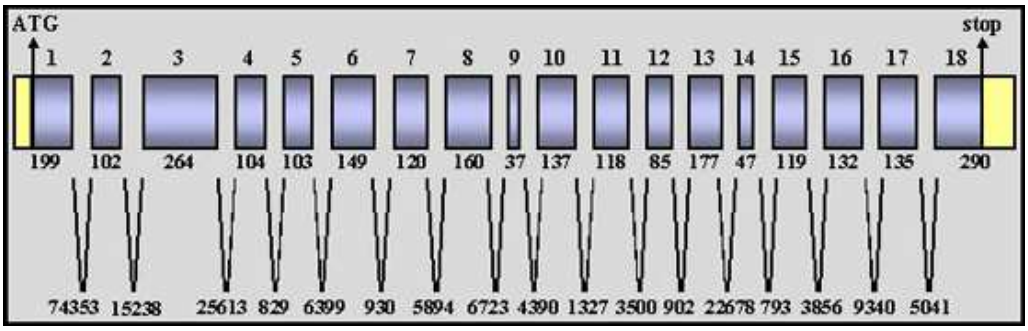

Diagram of the BRAF gene. Exons are represented by boxes (in scale) transcribed and untranscribed sequences in blue and yellow, with exon numbers on top and number of base pairs at the bottom. Introns are represented by black bars (not in scale) and the number of base pairs indicated. The arrows show the ATG and the stop codons respectively

BRAF-activating missense point mutations in the kinase domain are clustered in exons 11 and 15 of the gene and the T1799A transversion mutation accounts for more than 80% of the more than 40 mutations identified in *BRAF* gene (20). The T1799A mutation results in a V600E (formerly designated V599E) amino acid substitution in the protein product and subsequent constitutive activation of the BRAF kinase. The V600E mutation is thought to mimic phosphorylation in the activation segment of BRAF by inserting a negatively charged residue adjacent to an activating phosphorylation site at Ser-599 (16). This is believed to cause the conversion of BRAF to a catalytically active form by disrupting the association of the activation segment with the ATP-binding P loop, which normally holds BRAF in an inactive confirmation (18, 19).

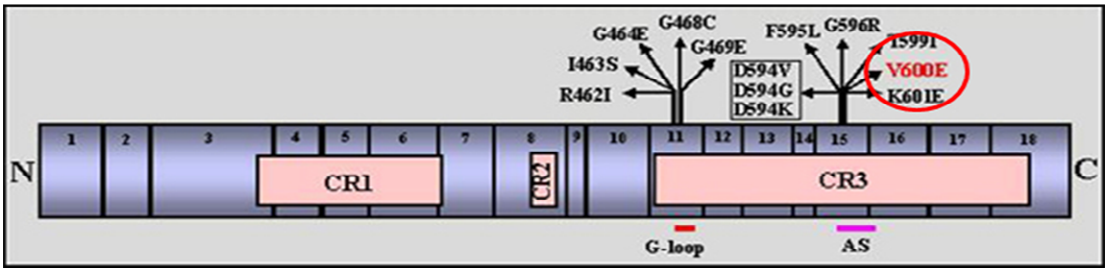

Diagram of the BRAF protein in scale. Numbers inside the blue boxes indicate the exon from which is translated each part of the protein. The three boxes inside represent the conserved regions of the protein with the ARAF and RAF-1 genes (CR1, CR2 and CR3). With green bars are represented three different domains: RBD (Ras binding domain), CRD (Cysteine-rich domain) and KD (Kinase domain). A conserved glycine motif (G-loop) in exon 11 is indicated with a red bar and the activation segment (AS) in exon 15 with a pink bar. The black arrows indicate the major phosphorylation sites of the protein. C: Carboxyl-terminal; N: Amino-terminal.

Discovery and characterization of the T1799A *BRAF* mutation in thyroid cancer represent one of the most exciting advances in the molecular biology of thyroid cancer in recent years (21). In fact, this mutation is the most common known genetic alteration in thyroid cancer. A few other activated BRAF mutants are only rarely found in thyroid cancer. These include the BRAF K601E (22), AKAP9-BRAF (23), BRAF V600E+K601del (24), BRAF V599ins (25), and V600D+FGLAT601-605ins, which results from an insertion of 18 nucleotides at nucleotide T1799. Thus, the T1799A mutation is the most common and virtually the only *BRAF* mutation identified in thyroid cancer. Xing et al. showed that $BRAF^{V600E}$ mutation was not a germline mutation in familial nonmedullary thyroid cancers (26), and, as a somatic genetic alteration, occurs exclusively in PTC and PTC-derived ATC, with an average prevalence of about 45% in the former and 25% in the latter; it does not occur in FTC or other types of thyroid tumors (2). Transgenic mouse model (27), cell line and xenograft tumor studies (28) demonstrated the tumorigenic ability of $BRAF^{V600E}$ and its requirement to maintain cancer cell growth and proliferation.

Many studies have investigated the relationship of $BRAF^{V600E}$ mutation with clinicopathological characteristics of PTC (29). Although the results are not entirely consistent, most of the studies from various ethnic and geographical backgrounds demonstrate a significant association of $BRAF^{V600E}$ with one or more conventional high-risk clinicopathological characteristics of PTC. For example, three recent studies — from the United States (30), Spain (31), and Italy (32) — have all demonstrated a significant association of $BRAF^{V600E}$ with extrathyroidal invasion and advanced stages. Association of $BRAF^{V600E}$ with lymph node metastasis was also reported in the Italian study (32). Consistent with the role of $BRAF^{V600E}$ mutation in lymph node metastasis of PTC, several studies observed a high prevalence of this mutation in lymph node-metastasized PTC (33, 21). Interestingly, in these studies $BRAF^{V600E}$ was sometimes found to be in the lymph node-metastasized PTC but not in the primary tumors, raising the possibility that this mutation could occur *de novo* in PTC cells metastasized to lymph nodes. To further support a role of $BRAF^{V600E}$ in lymph node metastasis of PTC, Rodolico *et al.* (34) recently demonstrated that metastatic PTC lesions in lymph nodes harboring *BRAF* mutation were larger in size than those harboring wide-type alleles. This study also showed a higher prevalence of extracapsular invasion of metastasized lymph nodes with $BRAF^{V600E}$ than metastasized lymph nodes without the mutation.

Xing et al. demonstrated an interesting association of $BRAF^{V600E}$ with loss of radioiodine avidity in recurrent PTC and its failure to be cured (35). This is consistent with finding of BRAF mutant-promoted silencing of thyroid iodide-handling genes and the reversal of this process by silencing the expression of BRAF mutant in thyroid cells (36).

Numerous studies demonstrated a close association of $BRAF^{V600E}$ with dedifferentiation of PTC as reflected by decreased expression of thyroid-specific genes in PTC, including *NIS* (37, 38), *TPO* (39), *pendrin* (40), and *Tg* (37). Therefore, BRAF mutation is a novel powerful molecular prognostic marker for poorer prognosis of thyroid cancer (2).

$BRAF^{V600E}$ has been reported to be responsible for both the initiation of tumorigenesis and its progression. PTC metastatic lesions in lymph nodes harboring $BRAF^{V600E}$ have been described as larger in size than those harboring wild-type alleles ($BRAF^{WT}$) (34). However, the exact molecular mechanisms determined by $BRAF^{V600E}$ have not been fully elucidated.

CHAPTER 3: Nuclear Factor (NF)-κB

An important signaling pathway often altered in human cancers is the IKK/NF-κB signaling module. Aberrant NF-κB regulation has been observed in many cancers, including both solid and hematopoietic malignancies,

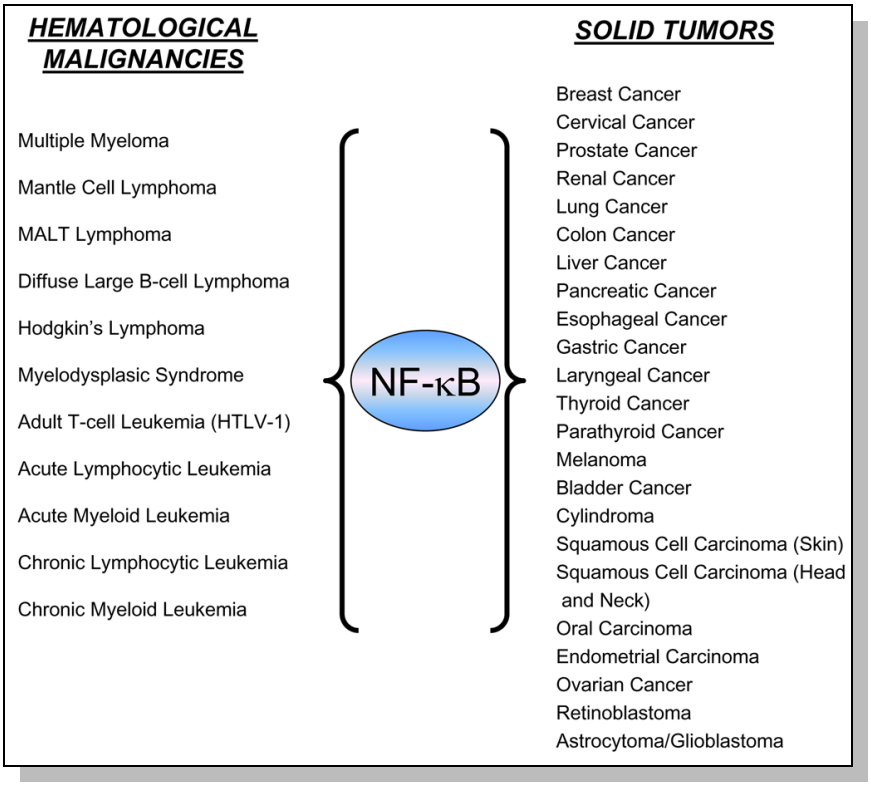

Human cancers that have been linked to constitutive NF-κB activation. Various hematological malignancies and solid tumors that exhibit constitutive NF-κB activation.

and NF-κB can affect all six hallmarks of cancer through the transcriptional activation of genes associated with cell proliferation, angiogenesis, metastasis, tumor promotion, inflammation and suppression of apoptosis (41-44).

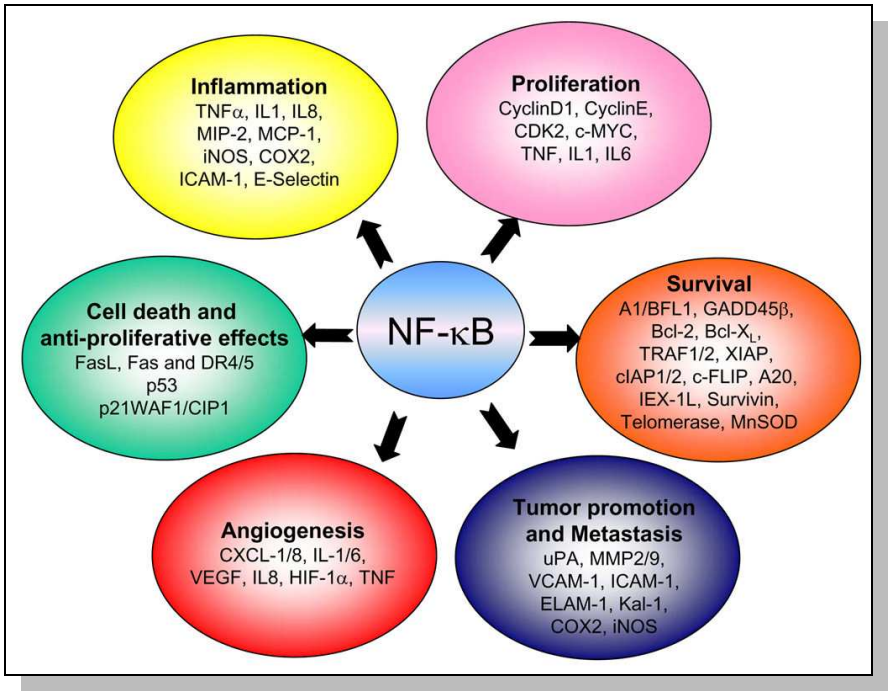

NF-κB target genes involved in cancer development and progression. NF-κB activation affects all six hallmarks of cancer through the transcription of genes involved in cell proliferation, angiogenesis, metastasis, inflammation and suppression of apoptosis as identified in both cell lines and tissue samples.

3.1 NF-κB transcription factors and their signaling pathways

In mammals, the NF-κB family is composed of five members, RelA (p65), RelB, cRel (Rel), NF-κB1 (p50 and its precursor p105) and NF-κB2 (p52 and its precursor p100) (45). These proteins form homo- and heterodimeric complexes, the activity of which is regulated by two major pathways.

The first one, known as the classical or canonical NF-κB activation pathway, mainly applies to RelA:p50 dimers, which, under non-stimulated conditions, are sequestered in the cytoplasm through interactions with inhibitory proteins of the IκB family. Following stimulation with a broad range of stimuli such as TNF-α or IL-1, viruses, genotoxic agents and ionizing radiation, the IκB molecules are phosphorylated by the IκB kinase complex (IKK) at specific serine residues, leading to their ubiquitination and degradation by the proteasome pathway. RelA:p50 dimers are subsequently released and free to translocate to the

nucleus where they activate transcription of various target genes (46). This pathway plays a major role in the control of innate immunity and inflammation (47).

The second pathway, the so-called alternative or non non-canonical NF-κB signaling pathway, is stimulated by a more restricted set of cytokines that all belong to the TNF superfamily (e.g. BAFF, CD40L and LTβ). This pathway involves the upstream kinase NF-κB-inducing kinase (NIK) which activates IKKα, thereby leading to the phosphorylation and proteasome-dependent processing of p100, the main RelB inhibitor, thus resulting in RelB:p52 and RelB:p50 nuclear translocation and DNA binding (48, 44). Most importantly, all studies point out to a crucial role for the alternative pathway in controlling the development, organization and function of secondary lymphoid organs and B-cell maturation and survival (49).

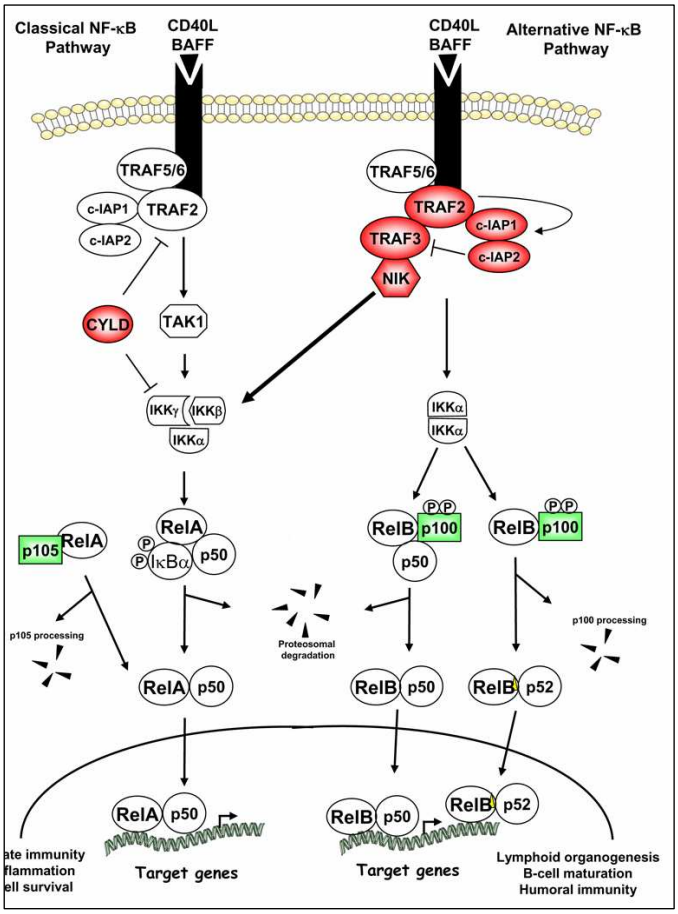

The classical and alternative NF-κB signaling pathways are represented downstream of CD40 and BAFF-R. Arrows indicate activating steps, and bars indicate inhibitory steps. Negative regulators subject to loss-of-function mutations are in red, and positive regulators affected by gain-of-function mutations are in green. Either type of mutations lead to NF-κB constitutive activation through NIK stabilization.

The activation of the canonical as well as the alternative NF-κB pathways relies on the inducible phosphorylation of IκB inhibitory proteins (IκBα for the classical pathway and p100 for the alternative pathway) by the IKK complex and its subunits (46). IKK is composed of two catalytic subunits, IKKα and IKKβ, and a regulatory subunit, NEMO/IKKγ. Disruption of genes encoding individual subunits has demonstrated that IKKβ and NEMO/IKKγ are required for activation of the classical NF-κB pathway by inflammatory signals, a pathway in which IKKα does not play an essential role. In contrast, RelB:p50 and RelB:p52 activation is absolutely dependent on IKKα, but not on IKKβ or NEMO/IKKγ (50).

NF-κB has been shown to play an important role in several tumors (51, 52), including thyroid cancer (53, 54).

3.2 NF-κB in cancer

The viral oncoprotein v-Rel had been identified as the causative agent of acute avian leukemia before discovery of NF-κB molecules (57). After NF-κB family proteins have been identified, many studies demonstrated the aberrant regulation of NF-κB signaling in a variety of human cancers including leukemia, lymphoma, head and neck squamous carcinoma, and ovarian, prostate, colon, breast and thyroid cancers (58, 59).

The genes encoding NF-κB family members p52/p100, c-Rel, p65 and IκB-like protein Bcl-3 are frequently rearranged or amplified in human lymphoma and leukemia, and inactivating mutations of IκBα gene can cause Hodgkin's lymphoma (60). Moreover, most oncogene products, including the Tax protein of human T-cell leukemia virus type 1 (HTLV-1), Bcr-Abl, Her-2/Neu and

oncogenic variants of Ras, can induce overexpression of p65 in cancer cells (61) and NF-κB activation (62).

The activation of NF-κB can contribute to the oncogenesis in several ways: by driving cell proliferation (63) perhaps through increased transcription of cyclin D1, which mediates G1/S progression of the cell cycle, by enhancing cell survival, and by promoting angiogenesis and metastasis (64).

Recently, it has been hypothesized that $BRAF^{V600E}$ promotes invasiveness of thyroid cancer cells via NF-κB activation (55, 56), but the exact BRAF-dependent mechanisms have not been established.

3.3 NF-KB and MAPK pathway in Papillary thyroid cancer

Several studies have suggested that the increased NF-κB activity is associated with thyroid carcinogenesis and tumor progression. A significant increase of p65 mRNA and protein expression, compared to normal thyroid cells, was found in thyroid cancer cell lines (65). Consistent with the elevated expression level, NF-κB DNA binding and reporter assays showed the increased transcriptional activities in the cultures of thyroid cancer cells (66). The activation of NF-κB was also observed in the papillary, follicular, and anaplastic cancer tissue specimens by immunohistochemical staining using an anti-p65 antibody (67). The products of *RET/PTCs*, activated mutant *RAS* and $BRAF^{V600E}$ genes involved in pathogenesis of papillary thyroid carcinoma can potently activate the MAPK pathway (68). In its turn, activated MAPK has been shown to induce activation of NF-κB signaling and associated NF-κB-mediated transcriptional activity (69). In addition, Palona et al. have observed that degradation of IκBα takes place shortly after ectopic accumulation of the $BRAF^{V600E}$ protein, resulting in the activation of NF-κB signaling via MEK-ERK independent pathway (55). In line

with these findings, previous study demonstrated that oncogenic Ret-induced NF-κB activity depends on IKK-mediated IκBα degradation and requires functional Ras, Raf and MEKK1 in a medullary thyroid cancer cell line TT, and that NF-κB activation is not accomplished by MEK/ERK activation (70).

CHAPTER 4: METALLOPROTEINASES (MMPs)

MMPs are proteolytic enzymes involved in extracellular matrix (ECM) and basement membranes (BMs) degradation (71). MMPs are physiologically linked to ovulation, blastocyst implantation, embryonic development and tissue morphogenesis. They also play an important role in tissue repair, wound healing, nerve growth, mammary gland development, as well as, angiogenesis and apoptosis (72).

ECM remodeling is also involved in pathologic conditions, such as inflammatory diseases or dermal photo aging (73). MMPs roles in pathology may be grouped into the following main types:

1. Tissue destruction, as in cancer invasion and metastasis, rheumatoid arthritis, osteoarthritis, decubitus ulcer, gastric ulcer, corneal ulceration, periodontal disease, brain injury and neuroinflammatory diseases;

2. Fibrosis, as in liver cirrhosis, fibrotic lung disease, otosclerosis, atherosclerosis, and multiple sclerosis;

3. Weakening of matrix, as in dilated cardiomyopathy, epidermolysis bullosa, aortic aneurysm and restenotic lesions (72).

Considering the main action mechanisms, MMPs roles may be discussed in terms of tissue destruction, cancer invasion and metastasis, angiogenesis, apoptosis, escaping mechanisms, and antitumor defensive mechanism, and as a pivotal role in the pathogenesis of arthritis, atherosclerosis, pulmonary emphysema, and endometriosis.

Currently, 25 different types of MMPs have been identified among vertebrates, 23 of them have been found in humans (73). The members of the MMP family have many similarities in their structure. All MMPs have a zinc-binding motif in

the catalytic domain. In addition, they have an N – terminal domain called predomain, followed by the propeptide domain. The majority of MMPs also have additional domains, e.g., Hemopexin domain. These additional domains are important in substrate recognition and in inhibitor binding (74).

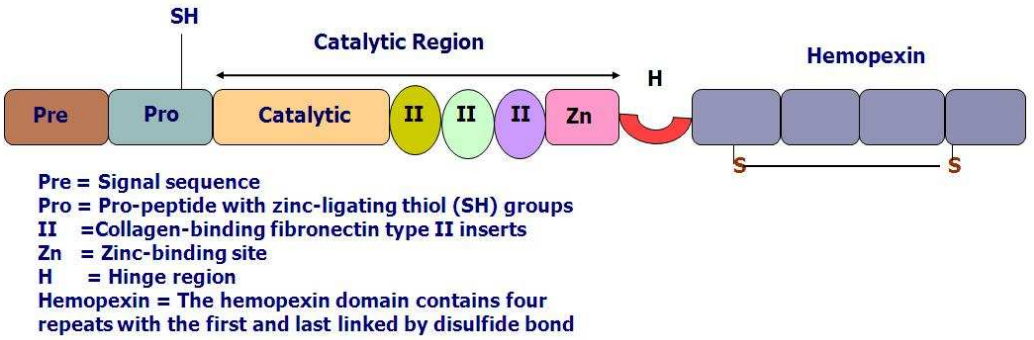

Basic domain structure of the gelatinases.

MMPs can be divided into subgroups according to their structure and substrate specificity. These subfamilies include collagenases, gelatinases, stromelysins, matrilysins, membrane-type MMPs (MT-MMPs) and other MMPs.

Class	MMP no.	Alternative name
Collagenases	MMP-1	Collagenase-1
	MMP-8	Neutrophil collagenase
	MMP-13	Collagenase-3
	MMP-18	Collagenase-4
Gelatinases	MMP-2	Gelatinase-A
	MMP-9	Gelatinase-B
Stromelysins	MMP-3	Stromelysin-1
	MMP-10	Stromelysin-2
	MMP-11	Stromelysin-3
Matrilysins	MMP-7 MP	Matrilysin PU
	MMP-26	Matrilysin-2
Membrane type (MT-MMPs)	MMP-14	MT1-MMP
	MMP-15	MT2-MMP
	MMP-16	MT3-MMP

	MMP-17	MT4-MMP
	MMP-24	MT5-MMP
	MMP-25	MT6-MMP
Other enzymes	MMP-12	Macrophage metalloelastase
	MMP-19	RASI 1
	MMP-20	Enamelysin
	MMP-21	Identified on chromosome 1
	MMP-22	Identified on chromosome 1
	MMP-23	From human ovary cDNA
	MMP-28	Epilysin
	MMP-29	Unnamed

***Table 1**. classification of vertebrates MMPs.*

The MMPs are regulated at many levels (75). The expression of MMPs genes are transcriptionally induced by oncogenic transformation, cytokines as well as, growth factors – including interleukins, interferons, EGF, KGF, NGF, VEGF, PDGF, TNF-α and TGF-β (76). The regulation of different MMPs also occurs at the protein level. MMPs are secreted as latent enzymes and this process can be achieved by activators and inhibitors. The expression of MMPs is primarily regulated at the level of transcription and their proteolytic activity requires zymogen activation. Many stimuli increase the expression of c-fos and c-jun protoncogene products and it's activate the activator protein-1 (AP-1) at proximal promoter regions of several MMPs such as MMP-1, -3, -7, - 9, -10, -12 and -13 types. Activity of AP-1 element is mediated by three groups of mitogen-activated protein kinases (MAPKs), which are ERK1/2, stress activated Jun N-terminal kinase and p38 MAPK (73). The proteolytic activities of MMPs are inhibited by Tissue Inhibitor of Metalloproteinases family (TIMP-1, -2, -3, -4) (77). TIMPs inhibit the activity of MMPs by binding to activated MMPs.

The role of MMPs in human cancer progression is supported by clinical evidence demonstrating a prognostic value for specific MMPs in several human cancers (78, 79).

Baldini et al. provided evidence demonstrating that normal thyrocytes constitutively express MMP-1, MMP-2, MMP-10, MMP-14 and TIMP-1, TIMP-2, TIMP-3, TIMP-4 and that this pattern of expression is modified in thyroid carcinoma derived cell lines [(follicular adenoma (HTU42), follicular carcinoma (FTC-133), papillary carcinoma (B-CPAP), and two different anaplastic carcinomas (CAL-62 and 8305C)]. In particular, they demonstrated that MMP-1, MMP-2, MMP-9, MMP-11, MMP-13 and MMP-14 are either increased or induced *de novo* in the different carcinoma cell types analyzed. Among these, MMP-11 and MMP-13 could be of interest as potential markers of thyrocyte transformation. In fact, their expression is absent in normal and follicular adenoma cell lines, while MMP-11 is induced in all the carcinoma cell lines studied and MMP-13 in all but one (80).

CHAPTER 5: TISSUE INHIBITOR OF METALLOPROTEINASE-1 (TIMP-1)

5.1 Metalloproteinase inhibitors

As their name implies, TIMPs are endogenous inhibitors of metalloproteinase activities and as such were initially thought to function principally to modulate matrix metalloproteinase activity and suppress extracellular matrix turnover. Recent studies have shown the importance of TIMPs during embryonic development, as well as the possible functional redundancy of some TIMPs in mammalian development (81). However, the study of TIMP function remains most closely associated with their role in tumor development and cancer progression.

The mammalian TIMP family has four members (TIMP-1, TIMP-2, TIMP-3 and TIMP-4), which share substantial sequence homology and structural identity at the protein level. The genes that encode human TIMPs are mapped on X-chromosome number Xp11.3 - Xp11.23, 17q25, 22q12.1-q13.2 and 3p25 respectively (82, 83). They show 30-40% similarity in structure at the amino acid level and possess 12 conserved cysteine residues required for the formation of six loops.

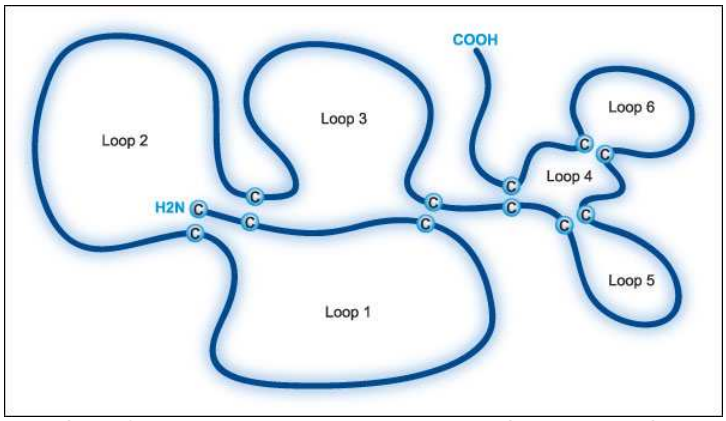

Schematic representation of TIMP-1 structure. TIMP1 contains 12 cysteine residues which form six loop structures through disulfide bonds. The N-terminus of TIMPs 1-4 binds to the catalytic domain of most activated MMPs and inhibits function. The C-terminus of TIMP1 and TIMP2 binds to the hemopexin domain of proMMP2 and proMMP9, respectively; this binding regulates MMP function.

TIMPs have basically two structural domains: an N-terminal domain consisting of six conserved cysteine residues forming three disulfide loops, which possesses MMP-inhibitory activity, and a C-terminal domain that also contains six conserved cysteine residues and forms three disulfide loops (84, 85). The overall structure of the N-terminal inhibitory domain is that of the oligosaccharide/oligonucleotide binding fold (OBfold) that is found in DNA or oligosaccharide binding proteins. This OB-fold is dominated by β-sheet structures separated by small flexible loop regions (85).

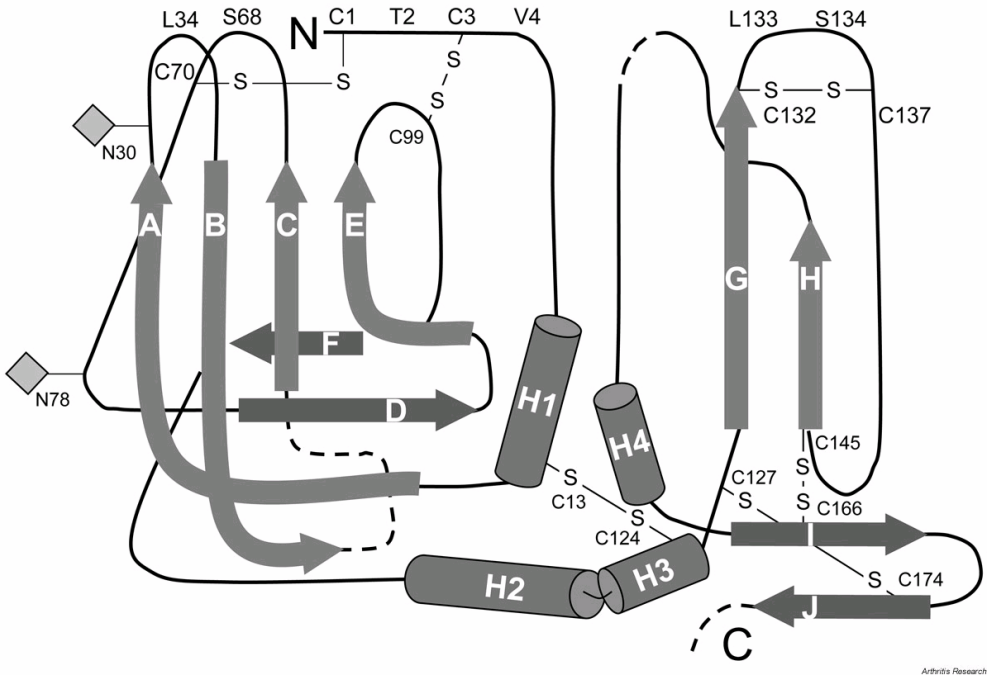

A schematic display of the secondary structure of tissue inhibitor of metalloproteinases 1 (TIMP-1). The crystal structure of TIMP-1 was determined as a complex with the catalytic domain of MMP-3. Strands (A–J) and helices (H1–H4) are shown. Two glycosylation sites are indicated by diamonds.

TIMP-3 specifically interacts with sulfated glycosaminoglycans and as a result is sequestered in the extracellular matrix (86), whereas the other TIMP family members remain soluble and diffusible.

Although the four members of the TIMP family are very similar in structure, they present marked differences in their expression pattern. While TIMP-2 expression is constitutive and ubiquitous, TIMP-1, -3 and -4 expression is inducible and tissue specific. TIMP-1 is mainly expressed in the reproductive system; TIMP-3 in the heart, kidney, and thymus, and TIMP-4 in heart, kidney, pancreas, colon, testes, brain and adipose tissue (87, 88). TIMP genes have been found in species ranging from *Caenorhabditis elegans* to humans, suggesting an important and conserved role in metazoans (89). Interestingly, TIMP-1, 3 and 4 genes are nested within introns of the synapsin gene family (90). Since synapsins are neuronal-specific phosphoproteins involved in synaptogenesis and neurotransmitter release, it is possible that TIMPs could have a regulatory role in the brain. Characterization of mouse TIMP-4 promoter showed potential sites for myogenin, GATA and Ets family members. Interestingly, it lacks AP1 or AP2 sites, which are involved in the inducible and basal expression of TIMP-1, -2 and -3 genes (90).

TIMPs can be regulated at the transcriptional level by various cytokines and growth factors, resulting in tissue-specific, constitutive, or inducible expression (91). Analysis of the *TIMP* promoters reveals that the *TIMP-2* promoter contains several Sp1 sequences characteristic of housekeeping genes, a finding consistent with the constitutive pattern of TIMP-2 protein and mRNA expression observed in adult murine tissues (92, 84).

5.2 TIMP-1

The primary structure of TIMP-1 was deduced from cDNA sequencing (93). There are four TIMPs which are homologous to each other and consisting of 184–194 amino acids with 12 conserved cysteines. The determination of the six

disulfide bond arrangement of TIMP-1 indicated that it consists of an N-terminal domain and a C-terminal domain, each containing three disulfide bonds (94). The N-terminal domain alone is fully functional for MMP inhibition (95). *TIMP-1* differs from the other members of the family in having a short exon 1 that is transcribed but not translated. The function of exon 1 appears related to the control of the specificity of tissue expression and may contain tissue-specific repressor elements (96).

TIMP regulation of cell fate is a highly complex process whose interpretation is further complicated by the indirect effects of TIMP-mediated inhibition of MMP activity. Moreover, there are numerous conflicting reports of TIMP effects on the same cellular process. Recent studies have begun to identify signaling pathways involved in the MMP-dependent growth-promoting effects of TIMP-1.

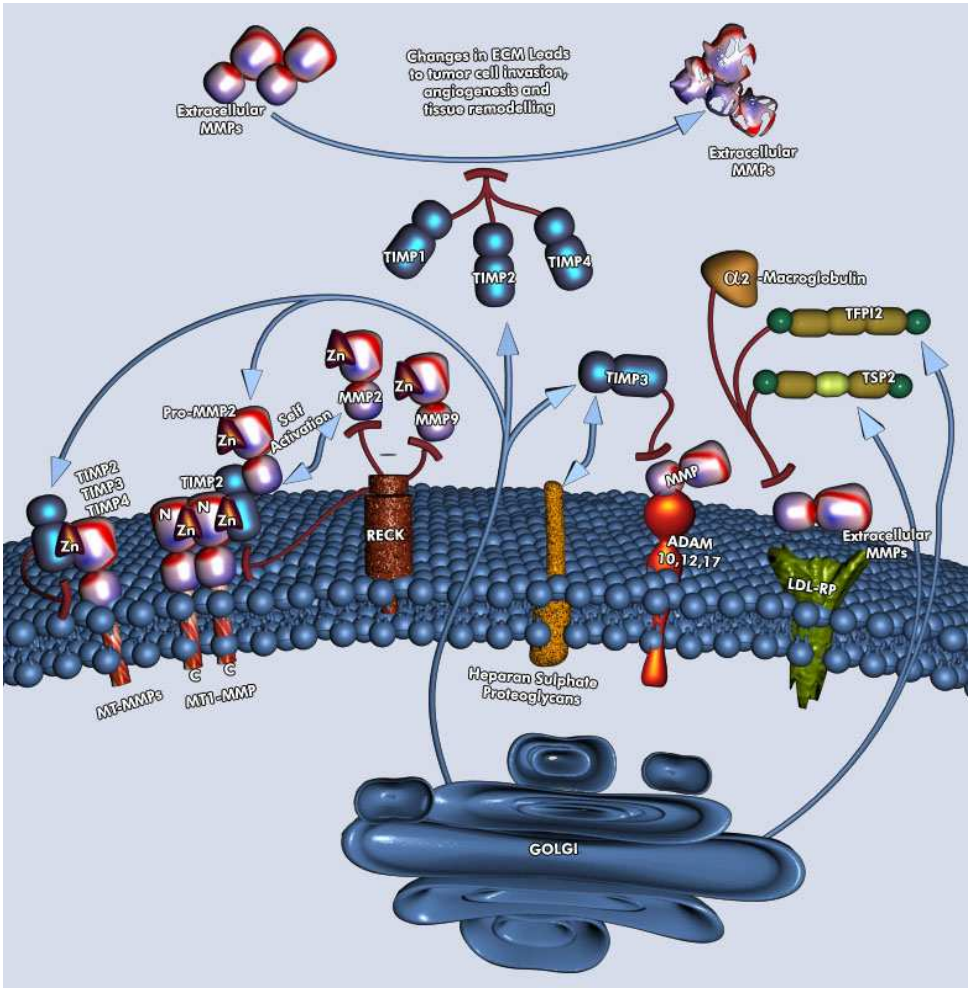

Four TIMPs have been identified (TIMP1,TIMP2. TIMP3 and TIMP4),each with its own physiologic role. TIMP1,TIMP2,and TIMP4 are found in a soluble form,while TIMP3 is anchored to the ECM by binding to heparan-sulphate-containing proteoglycans and possibly chondroitin-sulphate-containing proteoglycans. All four TIMPs inhibit active forms of all MMPs.

For instance, TIMP-1 specifically enhances the formation and growth of micrometastases in the liver (97). This effect is mediated through both the induction of hepatocyte growth factor (HGF) and the suppression of shedding its cognate receptor, cMet. It has been proposed, but not directly demonstrated, that the latter effect depends on inhibition of ADAM-10-mediated shedding of cMet. Thus high TIMP-1 expression in the liver creates a microenvironment that is conducive to tumor dissemination, and explains the observation that synthetic metalloproteinase inhibitors enhance formation of liver metastasis through inhibition of cMet shedding (84).

This research contrasts with reports that TIMP-1 inhibits MMP-mediated activation of HGF in the extracellular matrix and consequently reduces hepatocyte proliferation in a model of murine liver regeneration (98), and that TIMP-1 inhibition of MMP-mediated degradation of insulin-like growth factor (IGF) binding protein-3 (IGFBP-3) reduces bioavailability of IGFII, resulting in reduced growth of simian virus 40 (SV40) large T antigen-induced hepatocellular carcinoma (99).

These three studies emphasize the complexities of TIMP-associated cell signaling and the importance of recognizing that the observed effects of TIMPs on cell fate are highly dependent on the cellular context and details of the specific model system utilized (84).

TIMP-1 gene has been reported to be up-regulated in thyroid tumors (100). Notably, in other tumors TIMP-1 is thought to exert functions which are

independent of MMP inhibition, such as stimulation of proliferation and inhibition of apoptosis (84).

In 1989, Khokha *et al*. demonstrated that suppression of the endogenous TIMP-1 with antisense RNA conferred an oncogenic phenotype in Swiss 3T3 cells (101). This was the first suggestion that TIMPs may present an intrinsic barrier to tumor progression. Subsequently, many laboratories observed that most human malignancies were associated with increased matrix metalloproteinase (MMP) activity and that TIMPs could modulate the invasive activity and metastatic capacity of tumor cells (102). Retrospectively, it became apparent that the assumption that MMP activities were exclusively pro-invasive and necessarily facilitated tumor progression was naïve. It is now widely recognized that MMPs, like many other extracellular matrix (ECM) components, play a dual role in the process of tumor progression with both pro- and anti-tumorigenic activities (103). This dual role extends to the TIMPs. Although originally characterized by their ability to inhibit MMP activity, TIMPs have additional biological activities that are just beginning to be recognized and characterized. Over the past twenty years TIMPs have been shown to regulate a number of cellular processes including cell growth, migration, and apoptosis. Despite mounting evidence suggesting direct cell signaling capacity for the TIMPs, however, the requirement for MMP-inhibitory activity in mediating these cellular activities of the TIMPs remains controversial. Although TIMP-mediated inhibition of MMP activity is an important determinant of cell function, the concept of MMP-independent TIMP regulation of cell fate is now supported by the identification of specific cell binding partners -and specific signaling events- for TIMP family members. This is particularly relevant to the cell signaling mechanisms mediated by TIMP-1 and TIMP-2. The recognition of these MMP-

independent TIMP activities and understanding of the mechanisms involved have important implications for development of new therapies for cancer and other chronic diseases (84).

5.3 TIMP Functions Independent of MMP Inhibition

TIMP Promotion of Cell Growth

Several laboratories have reported that TIMP-1 promote cell division in various epithelial (keratinocytes), mesenchymal (fibroblasts), and tumor cell lines (104). Several distinct signaling pathways have been implicated in TIMP growth-promoting activity, including the mitogen activated protein kinase (MAPK) and adenosine 3′,5′-monophosphate (cAMP)-protein kinase A (PKA) pathways (105). The growth promoting activities of TIMP-1 may require activation of Ras, albeit by distinct pathways suggesting independent receptor mechanisms (106). Collectively these studies demonstrate that the functions of TIMPs are contextual; for instance, growth-promoting activity was only observed in the presence of free TIMPs, independent of MMP-binding or MMP inhibition.

TIMP Anti-apoptotic Activity

TIMP-1 expression inversely correlates with the susceptibility to induction of apoptosis in various human Burkitt's lymphoma cell lines (107). These studies demonstrated that treatment with recombinant TIMP-1 or forced expression of TIMP-1 in a TIMP-negative cell line reduces susceptibility to induction of apoptosis (intrinsic and extrinsic pathways).

TIMP-1 also inhibits apoptosis and anoikis (apoptosis induced by loss of cell adhesion) in human breast epithelial cells in vitro (108). Here, Bcl-2 overexpression increased the abundance of TIMP-1 protein in breast epithelial

cell lines (MCF10A and MCF7), whereas it has no effect on MMP or TIMP-2 expression. Furthermore, TIMP-1 overexpression suppresses anoikis in MCF10A cells. These findings show that the anti-apoptotic activity of TIMP-1 does not depend on its ability to stabilize cell-matrix interactions, and is independent of MMP inhibition. In this model system TIMP-1 activates the focal adhesion kinase (FAK)-phosphoinositol-3 kinase (PI3K) pathway to protect cells from intrinsic and extrinsic cell death (84). These studies indicate that TIMP-1 mediates activation of specific signal transduction pathways that protect cells from apoptosis in a fashion that is independent of its metalloproteinase inhibitory activity.

5.4 TIMP Receptor CD63

The high-affinity cell surface binding of TIMP-1 to myeloid leukemia cells and keratinocytes showed by Zhao WQ et al. suggested the presence of cellular binding partners (109). Recently, a yeast two-hybrid approach was used to identify CD63, a member of the tetraspanin family, as a cell-binding partner for TIMP-1 in MCF10A human mammary epithelial cells (110).

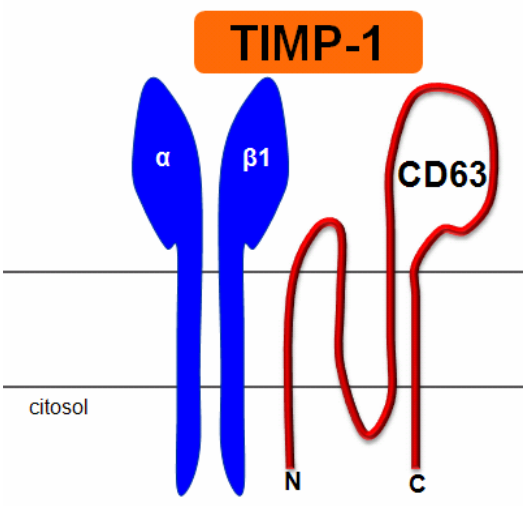

TIMP-1 interacts with the tetraspanin CD63, which associates with the β1 subunit of integrin receptors.

CD63 is a member of the tetraspanins, a group of hydrophobic proteins containing four transmembrane α-helices, two extracellular loops, and a short cytoplasmic tail. CD63 is present in late endosomes, lysosomes, secretory vesicles, and in the plasma membrane. At the plasma membrane, the members of the tetraspanin family including CD63 are known to interact with cell adhesion molecules such as integrins, regulating intracellular signal transduction pathways including cell adhesion, motility, and survival (110, 111, 112).

CD63 was first identified as a 40-kDa platelet-activating glycoprotein (Pltgp40) (113) and was found to be identical to ME491, an antigen associated with human malignant melanoma. A recent study reported increased CD63 expression on activated lymphocytes, especially on the cell surface where CD63 was suggested to function as a co-stimulatory signal to activate T cells and transmit cell survival signals when stimulated by anti-CD63 antibody (114).

TIMP-1 interaction with the tetraspanin member CD63 implies potentially diverse effects of TIMP-1 signaling on many cellular processes. Tetraspanins not only interact with integrins but also interact with many Ig superfamily proteins, complement regulatory proteins, growth factors, growth factor receptors, and signaling enzymes (115). The intracellular cytoplasmic tail of CD63 interacts with signaling molecules including phosphatidylinositol 4-kinases (PI4-k) and Src (116). Increasing evidence suggests that CD63 regulates FAK, Src, Gab2, PI3K, Akt, and PI4K signaling pathways as shown by modulation of these pathways upon anti-CD63 antibody binding to CD63 in breast carcinoma cells and immune cells. By binding to CD63, TIMP-1 may alter CD63 interactions with integrins within the tetraspanin microdomain and in turn influence integrin signaling. Alternatively, TIMP-1 binding to CD63 may

modulate recycling and redistribution of the integrin complex and/or regulate their activity, resulting in changes in signal transduction pathways (110).

TIMP-1 function is influenced by cellular context, specifically in that MMPs, in particular MMP-9, may reduce the effective concentration of TIMP-1 and compete with TIMP-1 for binding to the cell surface receptor CD63 (117). In contrast to TIMP-2, TIMP-1 concentrations are increased in cancer patients, particularly in those with breast or colorectal carcinoma, and this increase is negatively associated with patient outcome (118). These recent studies have demonstrated the clinical utility of TIMP-1 as a biomarker and independent prognostic factor in breast, colorectal, and several hematological cancers. They are consistent with the anti-apoptotic activity of TIMP-1 mediated by CD63 binding.

The identification of cell surface receptors for TIMP family members is a first step in beginning to sort out the MMP-independent, cytokine-like functions of the TIMPs. Hopefully, this could serve as a starting point for the molecular dissection of signaling events associated with the various activities of these proteins and their function in both normal physiologic and pathologic processes. It is clear that the pleotropic activities of the TIMP family members are complex and depend upon subtle interactions with other extracellular components, as well as direct interactions with cell binding partners. Understanding these processes and how they are modulated during disease progression will be helpful in development of novel therapeutic interventions (84).

CHAPTER 6: PI3K/AKT PATHWAY

6.1 The PI3K/Akt pathway in human cancers

Like the MAP kinase pathway, the phosphatidylinositol-3 kinase (PI3K)/Akt signaling pathway (PI3K pathway) plays a fundamental role in the regulation of cell growth, proliferation and survival and in human tumorigenesis (119). Upon activation by signaling from various membrane growth factor receptors, such as epidermal growth factor receptor (EGFR), platelet-derived growth factor receptor (PDGFR), vascular epithelial growth factor (VEGF) receptor, c-MET, and c-KIT, the p110 catalytic subunits (PIK3CA and PIK3CB) phosphorylate phosphatidylinositol-4,5-bisphosphate to produce phosphatidylinositol-3,4,5-trisphosphate (PIP3), which localizes the Ser/Thr kinase Akt to cell membrane where it becomes phosphorylated and activated by the phosphoinositide-dependent kinases (PDK), particularly PDK-1.

There are three types of Akts: Akt-1, Akt-2 and Akt-3. Activated Akt phosphorylates down-stream protein effectors and amplifies the signaling cascade, promoting cell proliferation and inhibiting apoptosis. Signaling of the PI3K/Akt pathway is antagonized by the tumor suppressor gene *PTEN* product, PTEN, which is a phosphatase that dephosphorylates PIP3, hence terminating the signaling of the PI3K/Akt pathway (120, 2). The *PIK3CA* gene frequently harbors mutations and amplifications in human cancers (121).

6.2 The PI3K/Akt pathway in thyroid cancer

Previous studies showed common activation of the PI3K signaling in thyroid cancers (122). Among the three isoforms of Akt, Akt-1 and Akt-2 were the most abundant and important in thyroid cancer (123). Some studies reported

genomic copy gain and amplification of the *PIK3CA* in thyroid tumors, particularly FTC and ATC (124). They have also shown that *PIK3CA* mutation is particularly common in ATC and is relatively uncommon but can occur in differentiated thyroid cancer. *Ras* mutation is commonly found in thyroid tumors, particularly FTC and BTA (125). Xing et al. have previously analyzed a number of genetic alterations in the PI3K pathway, including *PIKCA* mutation and amplification, *Ras* mutation, and *PTEN* mutation in various thyroid tumors, and found a relatively high prevalence of them, particularly in FTC and ATC (2). Coexistence of some of these genetic alterations and their coexistence with *BRAF* mutation were more frequently seen in aggressive thyroid cancers, particularly ATC (124). These studies have expanded these studies to a large panel of genetic alterations, including mutations and genetic amplifications, in about 20 genes in this pathway and found at least one genetic alteration in 46/48 (96%) ATC and co-existence of two or more genetic alterations in 37/48 (77%) ATC (126). Interestingly, genetic alterations that could activate both the MAP kinase and PI3K pathways were found in most (81%) ATC, which was in good correlation with elevated phosphorylation of ERK and Akt. These data provide the strongest genetic evidence for an extensive role of dual involvement of the MAP kinase and PI3K pathways in the pathogenesis of ATC, supporting a recent hypothesis that targeting multiple signaling pathways, particularly the MAP kinase and PI3K/Akt pathways, may be an effective and necessary therapeutic strategy for thyroid cancer (2).

BACKGROUND

Previously we investigated $BRAF^{V600E}$ mutation by real-time allele-specific amplification in 56 PTC nodules and their respective normal tissues. $BRAF^{V600E}$ was found in 22/28 classical variant (78.6%), 2/16 follicular variant (12.5%), 2/4 tall cell variant (50%), and 2/8 sclerosant variant (25%). $BRAF^{V600E}$ mutation was never detected in the healthy counterpart (non-tumoral tissue of the controlateral lobe). The clinical and histological characteristics are shown in table 2.

	$BRAF^{WT}$ No 28	**$BRAF^{V600E}$** No 28	**p**
	Mean ± SD	*Mean ± SD*	
Age	45.07±2.7	45.57±3.48	0.352
Sex	*(%)*	*(%)*	
Male	10 (35.7)	4 (14.3)	0.385
Female	18 (64.3)	24 (85.7)	
	Mean ± SD	*Mean ± SD*	
Tumor size (cm)	1.9 ± 1.4	1.4 ± 0.5	0.667
Histological variants	*(%)*	*(%)*	
Classical	6 (21.4)	22 (78.6)	0.007*
Follicular	14 (87.5)	2 (12.5)	
Tall Cell	2 (50)	2 (50)	
Sclerosant	6 (75)	2 (25)	

***Table 2**. Clinical and histological characteristics of PTCs (No 56) evaluated.*

56 PTC specimens collected for the Sicilian Registry of Thyroid Tumours were used for this study. They comprised tissue from tumoral nodules and from the respective controlateral healthy lobe. The histological variants 28 conventional/classical PTC, 4 tall cell PTCs, 16 follicular PTCs, and 8 sclerosant variant PTCs. The IRB of the University of Palermo, Italy, approved the study.

Microarray assay on $BRAF^{V600E}$ and $BRAF^{WT}$ PTC nodules and their respective healthy counterparts showed that $BRAF^{V600E}$ PTC nodules are characterized by *TIMP-1* up-regulation (4.03 ± 0.46 fold increase) in comparison to $BRAF^{WT}$ PTCs (0.98 ± 0.5 fold increase) ($p< 0.001$).

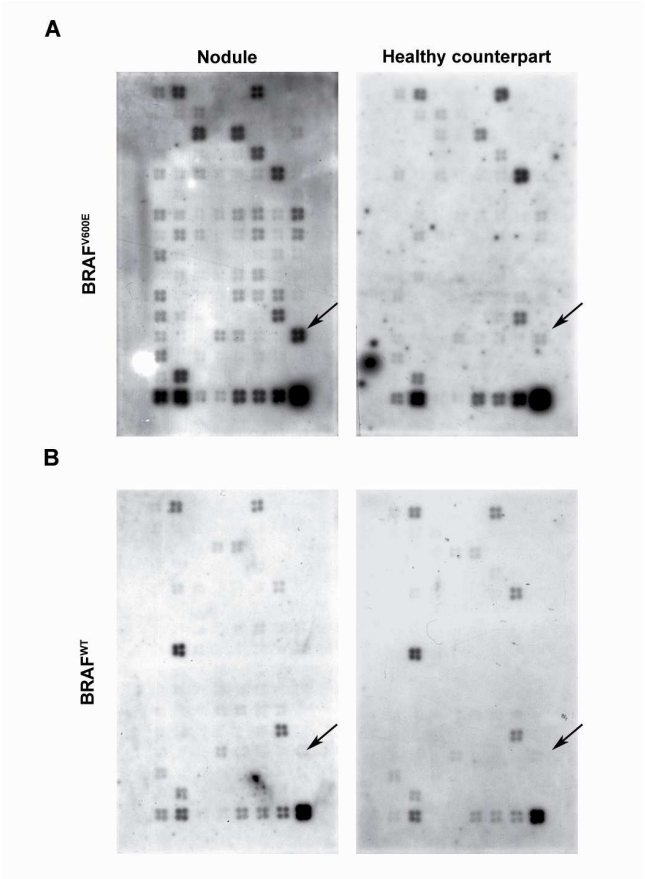

Microarray of TIMP-1 expression in $BRAF^{V600E}$ and $BRAF^{WT}$ PTCs and their healthy counterparts. TIMP-1 is significantly hyper-expressed in $BRAF^{V600E}$ nodule (left panel) in comparison to the healthy counterpart (right panel) (A), $BRAF^{WT}$ nodule (left panel) and in their healthy counterpart (right panel) (B); ($p<0.001$). Arrows indicate TIMP-1 position in the array. One representative experiment out of 6 oligonucleotide microarrays is shown.

Results were then validated by qRT-PCR in all 56 thyroid samples. PCR showed that TIMP-1 is significantly up-regulated in $BRAF^{V600E}$ nodules when

compared to their healthy counterparts (p<0.001). By contrast, no difference was found between $BRAF^{WT}$ nodules and their controlateral tissue (p=0.719).

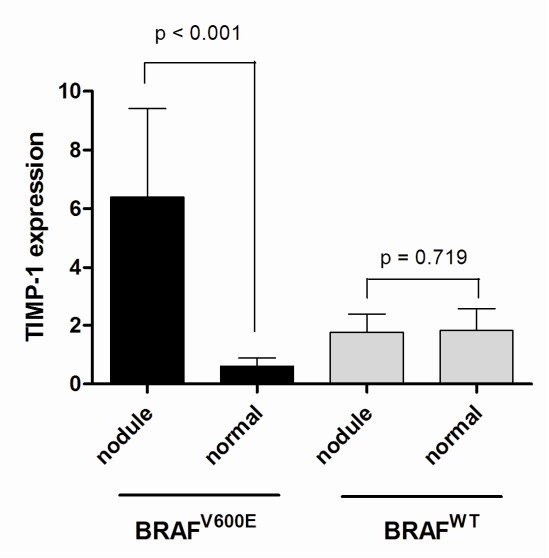

TIMP-1 qRT-PCR in 56 thyroid samples

These data were further confirmed by western blot analysis and immunohistochemistry.

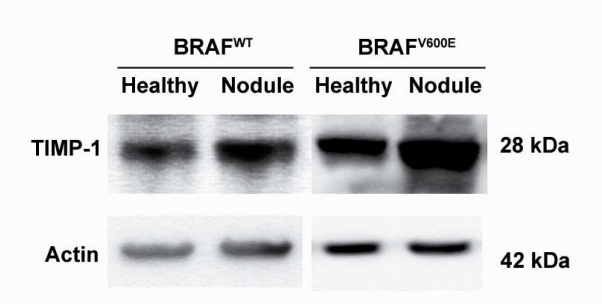

TIMP-1 western blot.
Densitometric analysis: $BRAF^{V600E}$ nodule 122.7 ± 6.7 vs $BRAF^{WT}$ nodule 40.9 ± 25.9; p< 0.001)

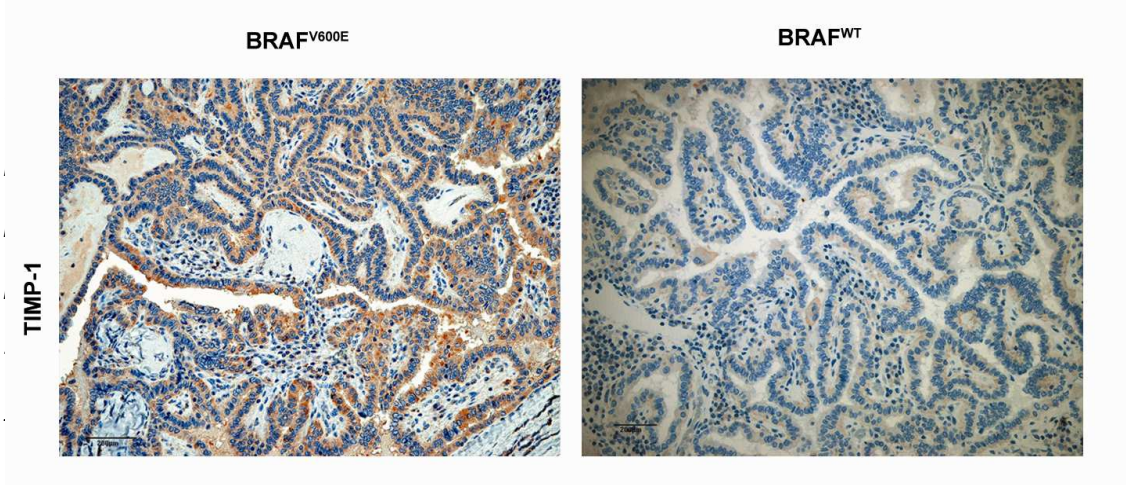

Immunohistochemistry in PTC samples.

Starting from this background, we focused our research on a possible molecular mechanism that could explain the association of $BRAF^{V600E}$ with high-risk clinicopathological characteristics of PTC, like extrathyroidal invasion, lymph node metastasis, and advanced disease stages.

Our aim was to evaluate whether an interplay among $BRAF^{V600E}$, TIMP-1 and NF-κB factors exerts a functional role in PTCs.

MATERIALS

AND

METHODS

Immunohistochemistry

5µm paraffin-embedded sections were analyzed for the expression CD-63. Briefly, tissue sections were deparaffinized, rehydrated and microwave-heated in 10mM sodium citrate buffer for antigen retrieval. Sections were then incubated with 3% hydrogen peroxide/PBS for 5 minutes, and blocked with 3% PBS/BSA. Incubation with mouse anti-human CD63 (sc-5275, Santa Cruz Biotechnology) was performed at room temperature for 1 hour. Expression was detected with secondary biotinylated antibodies, streptavidin/horseradish peroxidase and chromogen 3-amino-9-ethylcarbazole (AEC) substrate. Slides were counterstained with hematoxylin/eosin.

RNA extraction, RT-PCR and quantitative RT-PCR (qRT-PCR)

PTC specimens were frozen in RNA later (Sigma-Aldrich, Milan, Italy) and stored at -20° C until use. RNA was extracted using RNeasy Mini Kit (Qiagen, Milan, Italy) including a digestion step with DNase I set (Qiagen, Milan, Italy) according to manufacturer's instructions. RNA was reverse transcribed with Oligo-dT primers (Applied Biosystems, Darmstad, Germany) and Stratascript RT (Stratagene Amsterdam, Netherland), according to the manufacturer's protocol. Gene expression was analyzed by real-time quantitative PCR (qRT-PCR) with Quantitect SYBR Green PCR Kit (Qiagen, Milan, Italy) using a LightCycler 1.5 Instrument (Roche Diagnostics GmbH, Germany). Reactions were performed at least in triplicates. Specificity of the amplified products was determined by melting peak analysis. Quantification for each gene of interest was performed in relation to appropriate standard curve. Gene expression was normalized against the housekeeping gene *β-actin* which was stable among all the samples. PCR primers for TIMP-1 and BRAF genes were purchased from

Qiagen (Quantitect Primer Assay, Hs_TIMP-1_SG, QT00084168; Hs_BRAF_1_SG, QT00078176) while *β-actin* primers were purchased from Realtimeprimers.com. The PCR thermal cycler conditions were 95℃ for 15 minutes followed by 45 cycles of 95℃ for 15 secon ds, 55℃ for 15 seconds and 72℃ for 15 seconds.

DNA extraction and detection of BRAF^{V600E} mutation

DNA was extracted and purified using Qiagen DNAeasy Tissue Kit, according to the manufacturer's protocol (Qiagen, Milan, Italy). DNA quantity and quality was assessed by UV spectrophotometry. BRAF^{V600E} mutation was detected by real-time allele-specific amplification essentially as previously described (134).

Protein extraction and Western Blot analysis

Proteins were extracted from tissue samples or cell lines using RadioImmunoPrecipitation Assay (RIPA) buffer (50 mM Tris-HCl, pH 7.4, 150 mM NaCl, 1% Nonidet P40), supplemented with protease inhibitor cocktail (Complete mini, Roche, GmbH, Germany) and phosphatase inhibitors. Protein content was determined according to Bradford's method.

Proteins were separated by NuPAGE® 4-12% Bis-Tris Gel (Invitrogen, Milan, Italy), electrotransferred to nitrocellulose membranes, and blotted with the following primary antibodies: mouse anti human Tissue Inhibitor of Metalloproteinase-1 TIMP-1 (631661 MP Biomedical), mouse anti Raf-B F-7 IgG2a (sc-5284Santa Cruz Biotechnology), rabbit anti p-Akt1/2/3 Thr 308 (sc-16646-R Santa Cruz Biotechnology), rabbit anti Akt1/2/3 H-136 (sc-8312Santa Cruz Biotechnology,), mouse anti Bcl-2 IgG_1 (sc-7382Santa Cruz Biotechnology), rabbit anti Bcl-xL (sc-1041Santa Cruz Biotechnology), β-actin

(A5441Sigma-Aldrich, Milan, Italy). Secondary antibodies: Goat Anti-Rabbit IgG-HRP (sc-2030 Santa Cruz Biotechnology) and goat anti-mouse IgG-HRP (sc-2031Santa Cruz Biotechnology). The antigen–antibody complexes were visualized using the SuperSignal West Femto Maximum Sensitivity Substrate (Thermo Fisher Scientific) on a CCD camera (Chemidoc, Bio-Rad, Milan, Italy). The western blot bands were quantified with Quantity one software (Bio-Rad, Milan, Italy).

Gelatin zymography for MMP-9

Electrophoresis of 50 µg proteins was performed on 7.5% polyacrylamide gels containing gelatine (2 mg/ml) (Difco Lab) as previously described (*23*). Gels were rinsed twice in 2.5% Triton-X100, and incubated at 37℃ for 20 h in a buffer containing 0.2 M NaCl, 5 mM CaCl2, 50 mM Tris-HCl (pH 7.6), and 0.02% Briji-35 (Sigma-Aldrich, Milan, Italy). Gels were stained with 0.25% Coomassie blue, destained in 25% methanol and 10% acetic acid.

Electroforetic mobility shift assay (EMSA)

20 µg of total proteins were incubated with a double-stranded ^{32}P labelled oligonucleotide probe containing the specific recognition sequence for NF-κB (5'-AGTTGAGGGGACTTTCCCAGGC-3'), as previously described (127). Additionally, an unlabelled oligonucleotide was added in excess (100:1) to the labelled NF-κB probe, when appropriate for specific detection.

Cell cultures

BCPAP and TPC-1 cell lines were cultured in RPMI 1640 medium supplemented with 10% FBS, 5% penicillin-streptomycin and 5% glutamine.

KTC-1 cell line was cultured in Dulbecco's Modified Medium (DMEM) supplemented with 5% FBS, 5% penicillin-streptomycin and 5% glutamine. Cultures were maintained in 5% CO_2 at 37℃ in a humidified incubator.

siRNA Transfection

siRNAs were introduced into BCPAP cells using Interferin transfection agent (EuroClone, Milan, Italy), according to the manufacturer's instructions. Briefly, cells were seeded into six-well plate at a density of 300,000 cells/well or 96-well plate at a density of 7,000 cell/well. The transfection agent and the siRNA complex were added to the cells and incubated for 48 and 72 hrs. The final concentration of siRNA was 100 nM. Each assay was performed in triplicate in at least five independent experiments. *TIMP-1* was silenced using On target Plus Smart Pool Timp-1 siRNA (Dharmacon, L-011792-00). BRAF was silenced with using a chemically synthesized siRNA targeting $BRAF^{V600E}$ mutation (MU-A), as previously described (128*)*. siCONTROL, Non-Targeting siRNA pool was used as control (Dharmacon, D-001206-13).

Flow cytometry

Cells were incubated at RT for 30 min with mouse anti-human CD63 (Santa Cruz Biotechnology, sc-5275). After two washing steps with PBS, cells were incubated with goat anti-mouse IgG $F(ab)_2$ FITC (SantaCruz Biotechnology sc-3699). Cells were fixed with 4% paraformaldehyde for 10 minutes at room temperature than resuspended in permeabilization buffer containing 0.1% (w/v) saponin, 0.05% (w/v) NaN3 in Hanks' Balanced Salt Solution (HBSS). Cells were then incubated at RT for 30 min with PE-labeled monoclonal antibody for TIMP-1 (R&D Systems, IC970P, clone 635115). A negative control with an

isotype-matched antibody was included. After two washing steps with permeabilization buffer, cells were resuspended in PBS and analyzed on a FACSCalibur flow cytometer using CellQuest software (Becton and Dickinson).

Inhibition of NF-κB

BCPAP cells were plated in 6-well plate in 2 ml RPMI, stimulated for 24 hrs with 5 µM MG-132, 50 nM dexamethasone 21-phosphate (Sigma-Aldrich, Milan, Italy) and 10 µM parthenolide. Cells were then cultured for other 24 hrs with 30 µM monensin.

Treatment with recombinant TIMP-1

BCPAP cells were plated in 6-well plate in 2 ml serum free medium/well for 24 hrs and then incubated with 250 ng/ml of recombinant TIMP-1 protein (Calbiochem, PR019) for 30 and 60 minutes. Western Blot for Akt, p-Akt, Bcl-2, Bcl-xL were performed as described in the previous Section.

BCPAP cells were plated in a 96-well plate in 100 µl serum free medium/well and incubated with recombinant TIMP-1 protein up to 24 hrs at different concentration (5-250 ng/ml). Cell proliferation was assessed by colorimetric assay using BrdU (colorimetric) kit (Roche Diagnostics, GmbH, Germany). Invasion assay was performed as described below.

Regulation exerted by TIMP-1 on doxorubicin-chemoresistance

BCPAP cells were plated in a 96-well plate in 100 µl serum free medium/well. Cells were treated with 100 or 250 ng/ml rTIMP-1; 100 nM TIMP-1 siRNA; 100 nM BRAF siRNA; or TIMP-1 and BRAF siRNA combined. Cells were cultured with 2 µM doxorubicin up to 48 hrs. Cell proliferation was assessed by

colorimetric assay using 3-(4,5-Dimethylthiazol-2-yl)-2,5-diphenyltetrazolium bromide (MTT). Absorbance was read at 550 nm in a MultiskanFC microplate reader (Thermo Fisher Scientific). Apoptosis was evaluated by caspase-3 assay. Briefly, cells were fixed and permeabilized with Cytofix-Cytoperm kit (BD Pharmingen) according to the manufacturer's instructions. Data were analyzed with CELLQuest Pro software (Becton Dickinson Immunocytometry Systems). Gating was implemented based on negative control staining profiles.

Invasion Assay

BD BioCoat Matrigel™ invasion chambers (BD Biosciences) were rehydrated just before the assay using FBS-free RPMI according to the manufacturer's instructions. For silencing assay, BCPAP cells were silenced with MU-A (specific for $BRAF^{V600E}$) or with TIMP-1 siRNA and siCONTROL siRNA for 48 hrs, as above described. For rTIMP-1 and Akt inhibitor treatments, cells were directly plated on invasion chamber with 250 ng/ml rTIMP-1 for 24 hrs.

Cells were harvested by trypsinization, counted and suspended in RPMI containing 0.1% BSA. 5×10^5 cells/0.5 ml cells were added to the invasion chamber. Inserts were transferred into the wells of 24-well plate with 750 µL culture medium containing 5% FBS as chemoattractant. The assembled chambers were incubated for 24 hrs at 37℃. At the end of the incubation period, non migrating cells, which remained on the upper surface of the filter, were completely removed by wiping with a cotton swab. Cells on the underside of the insert were stained with 2.5 µg/ml of Hoechst33342 (Sigma-Aldrich, Milan, Italy) for 30 minutes at 37℃. Then the insert were observed using the Inverted Microscope Leica DM IRB and acquired with the Leica Qfluoro software. Quantification of invading cells was performed by counting

Hoechst33342-stained nuclei in 5 random fields. Analysis was performed with an image analysis software (Fiji software). A minimum of three inserts was utilized for each sample to assess invasion

Akt inhibition

BCPAP were treated with 10 µM Akt Inhibitor VIII Isoenzyme selective Akti-1/2 (Calbiochem) for 4 hrs to perform p-Akt and Akt western blot assays. BCPAP were also treated with 10 µM Akt Inhibitor for 24 hrs to perform both invasion assay by using BD BioCoat Matrigel™ invasion chambers (BD Biosciences) as described above, and cell proliferation assay by colorimetric assay using BrdU (colorimetric) kit (Roche Diagnostics, GmbH, Germany).

Statistical analysis

Continuous variables are represented as mean ± standard deviation (SD). Rates and proportions were calculated for dicotomic data and differences were analyzed by χ^2 test and Fisher exact test when appropriated. As continuous variables we used nonparametric tests, and differences were analyzed by the Mann-Whitney U-test. Differences between paired continuous variables (mRNA expression of TIMP-1, in nodule vs tissue) were analyzed by means of the Wilcoxon test. $P < 0.05$ was considered statistically significant. All analyses were performed with Statistical Package for Social Science (SPSS for Windows, v. 11.0; Chicago, Ill).

RESULTS

NF-κB is hyperactivated in PTC nodules harboring BRAF^{V600E} mutation and not in the healthy counterparts. NF-κB signaling pathway has been described as being upregulated in BRAF^{V600E} tumors (54), including PTCs (71%) (128). The mutation has been associated with more aggressive histology/behavior. Concerning the underlying mechanism, BRAF^{V600E} apparently promotes activation of NF-κB independently of downstream MAPK signaling (129). However, no precise correlation has been found between increased NF-κB activation and degree of malignant phenotype. Hence we investigated NF-κB activation in mutated and wild-type PTCs by Electrophoretic Mobility Shift Assay (EMSA). We found that NF-κB binding activity is increased in BRAF^{V600E} nodules in comparison to both BRAF^{WT} nodules and healthy counterparts (Fig. 1). Thus, our findings confirmed NF-κB system is an important pathway involved in BRAF^{V600E} PTC.

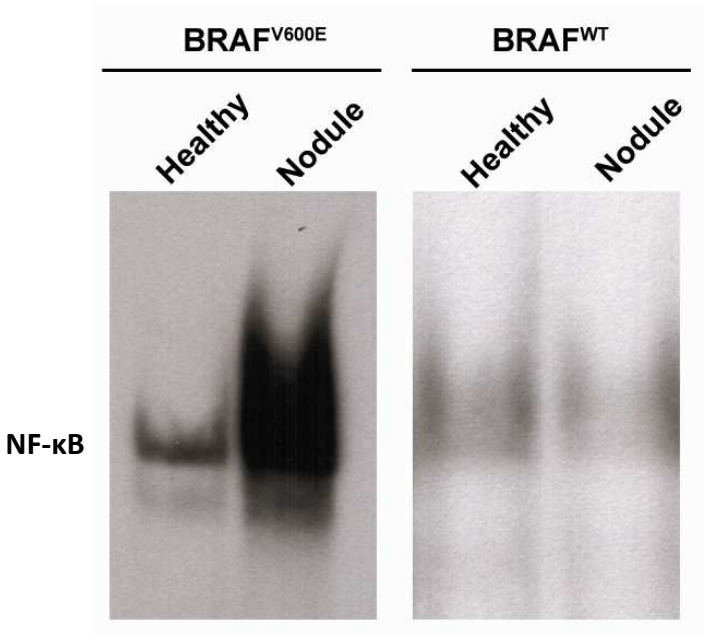

***Figure 1**. EMSA analysis showed that NF-κB binding activity is increased in BRAF^{V600E} nodules in comparison to both BRAF^{WT} nodules and healthy counterparts. Figure show one representative experiment.*

MMP-9 is hyperactivated in PTC nodules harboring BRAF^{V600E} mutation and not in the healthy counterparts. Tumor invasion is mediated by the action of MMPs, which are more expressed in tumor thyroid cells (129). Metastasis formation is more common in BRAF^{V600E} PTCs (*4*). Indeed, MMPs over-expression has been induced upon expression of BRAF^{V600E} in several thyroid cell lines (130).

We investigated the expression of MMPs in our PTCs by zymography. We observed higher proteolytic activity of MMP-9 in BRAF^{V600E} nodules in comparison to both BRAF^{WT} nodules and their healthy counterparts (Fig. 2). Therefore, our findings support the role of MMP system in mediating BRAF^{V600E} mutation-promoted progression of PTC.

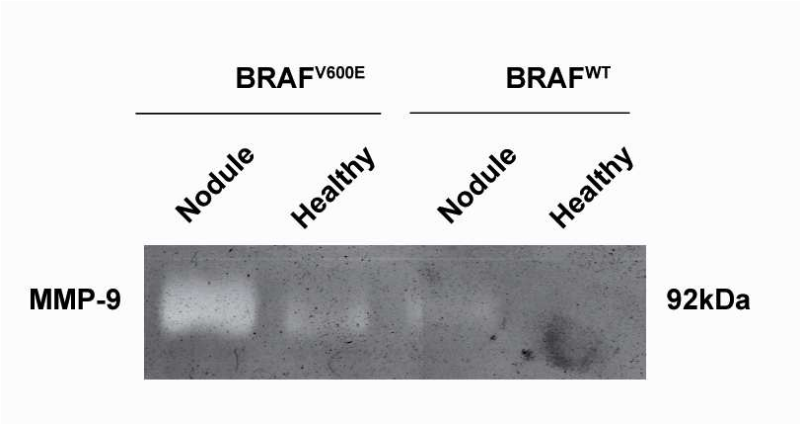

***Figure 2**. Zymography shows higher proteolytic activity of MMP-9 in BRAF^{V600E} nodules in comparison to both BRAF^{WT} nodules and their healthy counterparts.*

CD63 receptor is up-regulated in PTC nodules harboring BRAF^{V600E} mutation and not in the healthy counterparts. CD63, a member of the tetraspanin family, has been indicated as the TIMP-1 receptor in MCF10A human mammary epithelial cells (69). CD63 acts as a regulator of PI3K, FAK, Src, and Akt signaling pathways, which are implicated in the anti-apoptotic

activity of TIMP-1 (131). Immunohistochemistry analysis confirmed higher expression of CD63 in $BRAF^{V600E}$ in comparison to $BRAF^{WT}$ nodules (Fig. 3).

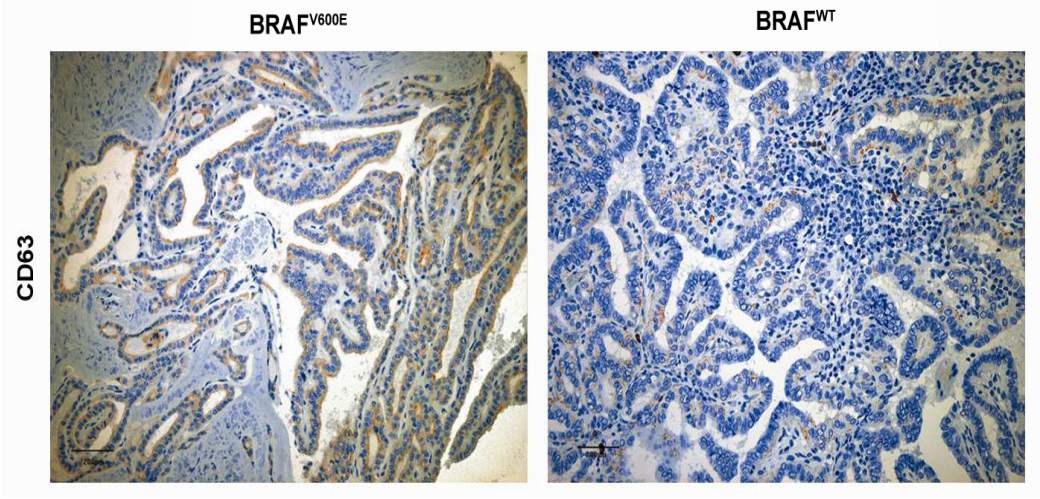

***Figure 3**. TIMP-1 receptor CD63 is hyper-expressed in $BRAF^{V600E}$ PTC (left) in comparison to $BRAF^{WT}$ PTC (right). Scale bar 200 μm. One representative experiment.*

Proof of the principle

We hypothesized that a relationship exists between $BRAF^{V600E}$, TIMP-1 hyper-expression and NF-κB activation. To validate this hypothesis we used well-established thyroid cell lines harboring or not harboring $BRAF^{V600E}$ mutation (132). We found that TIMP-1 mRNA expression was significantly higher in BCPAP cell line ($BRAF^{V600E/V600E}$) in comparison to KTC-1 ($BRAF^{V600E/WT}$) and TPC-1 ($BRAF^{WT/WT}$) cell lines, and normal thyroid mRNA (Fig. 4).

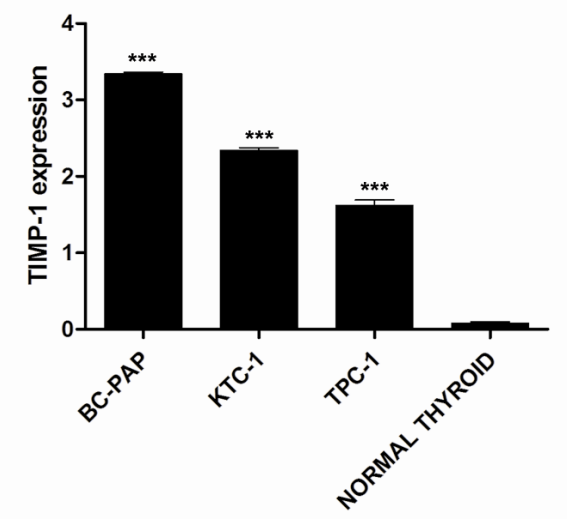

***Figure 4**. qRT-PCR shows that TIMP-1 is more expressed in BCPAP ($BRAF^{V600E/V600E}$) and KTC-1 ($BRAF^{V600E/WT}$) in comparison to TPC-1 cell line ($BRAF^{WT/WT}$) and normal thyroid (BCPAP, KTC-1 vs TPC-1 and normal thyroid; *** p <0.001)*

Flow cytometry confirmed BCPAP cells co-express TIMP-1 and CD63 (75.6 ± 3.2%) (Fig. 5).

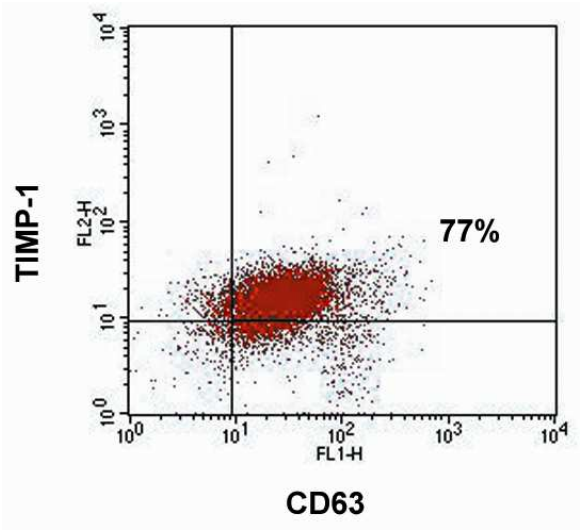

***Figure 5**. Flow cytometry analysis confirms TIMP-1 and CD63 co-expression in BCPAP cell line (mean ± SD: 75.6 ± 3.2%)*

Thus, BCPAP cell line was considered a suitable and reproducible in vitro system for testing our hypothesis. To verify the relationship between $BRAF^{V600E}$, NF-κB and TIMP-1, we silenced BRAF gene in BCPAP cell line using a specific small interfering RNA (siRNA) for the mutated form (MU-A). MU-A is incorporated into the RNA-induced silencing complex, which targets BRAF mRNA to prevent its translation. Silencing efficacy is shown in Fig. 6A-B.

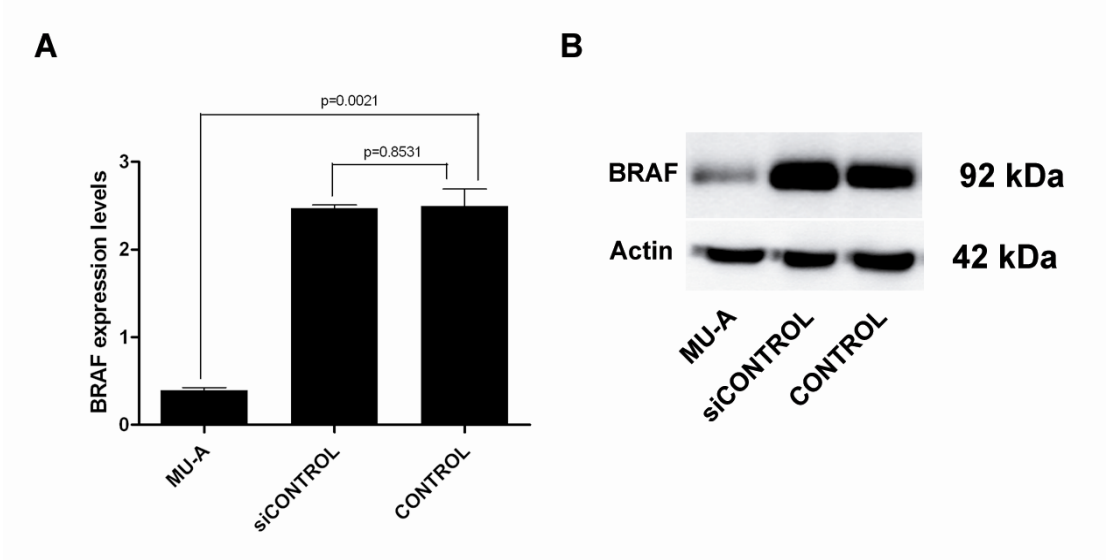

***Figure 6**. Silencing with a chemically synthesized siRNA targeting BRAF^{V600E} mutation (MU-A) determines decrease in BRAF mRNA and protein. **(A)** qRT-PCR shows that MU-A reduces BRAF expression in comparison to untreated cells (p = 0.0021). Data are normalized against β-actin gene expression. **(B)** Western-blot analysis shows that MU-A decreases BRAF expression in comparison to scrambled siRNA (siCONTROL) and untreated cells.*

We next performed an EMSA for NF-κB activation. We found a marked reduced NF-κB binding activity at 72 hrs after silencing, thus confirming that NF-κB is regulated by BRAF^{V600E} (Fig. 7A). At the same time points, qRT-PCR showed that TIMP-1 expression was significantly decreased in MU-A treated cells (p=0.0285) (Fig. 7B).

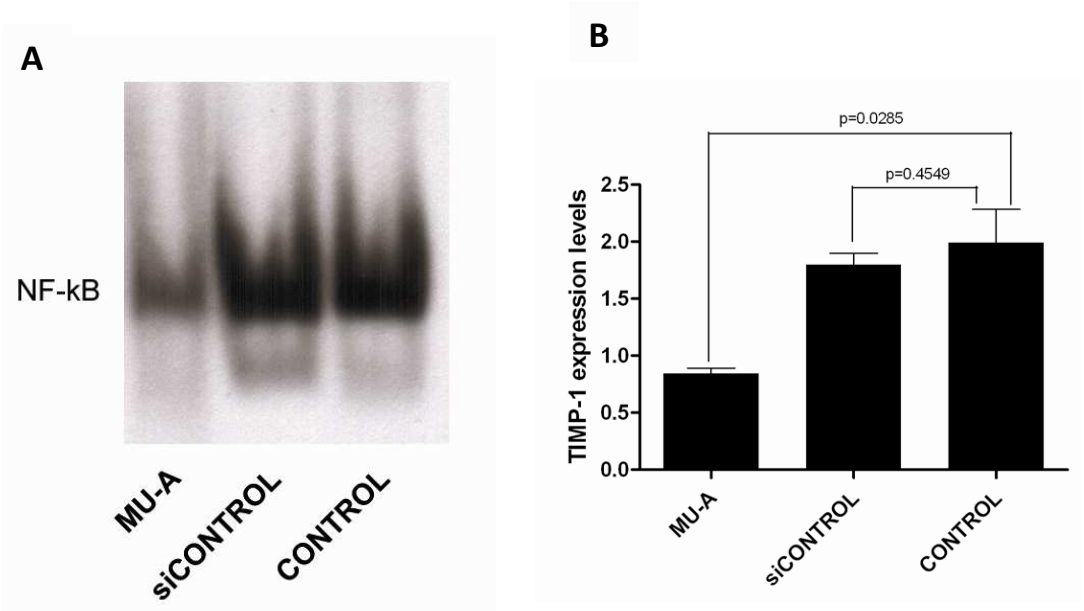

***Figure 7**. BRAF^{V600E} silencing results in reduction of NF-κB binding activity and TIMP-1 expression. **(A)** EMSA shows that MU-A decreases NF-κB binding activity in comparison to both siCONTROL and untreated cells. **(B)** qRT-PCR shows that MU-A reduces TIMP-1 expression in comparison to siCONTROL and untreated cells (p=0.028). (A) and (B): data are representative of at least three independent experiments.*

Furthermore, we evaluated whether BRAF^{V600E} inhibition can affect invasion in MU-A treated BCPAP cells. After 24 hrs in a BioCoated MatrigelTM chamber, MU-A treated cells decreased significantly their ability to invade (Fig. 8A and

8B), thus proving BRAF^{V600E} mutation exerts a pivotal role in regulating both NF-κB activation, TIMP-1 expression and tumor invasion.

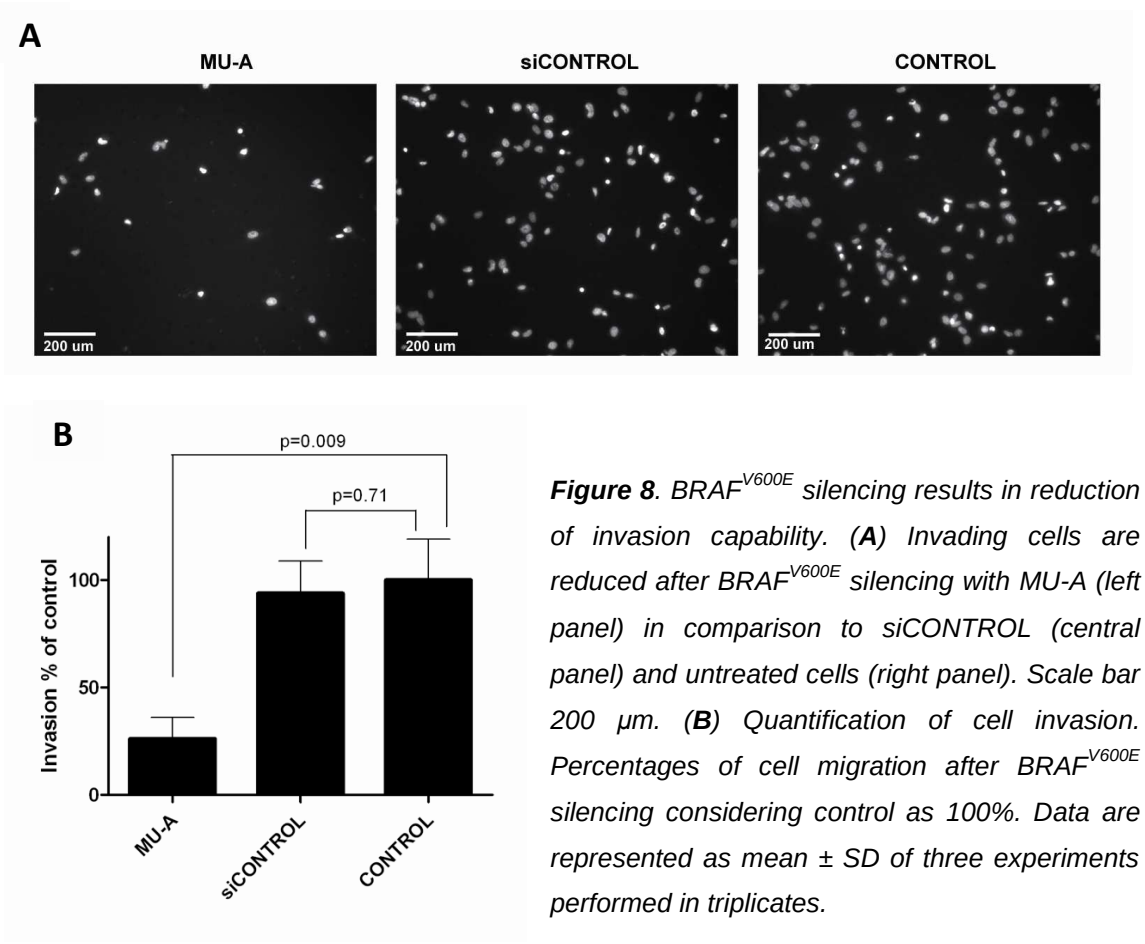

***Figure 8**. BRAF^{V600E} silencing results in reduction of invasion capability. (**A**) Invading cells are reduced after BRAF^{V600E} silencing with MU-A (left panel) in comparison to siCONTROL (central panel) and untreated cells (right panel). Scale bar 200 μm. (**B**) Quantification of cell invasion. Percentages of cell migration after BRAF^{V600E} silencing considering control as 100%. Data are represented as mean ± SD of three experiments performed in triplicates.*

To confirm our hypothesis, that is the relationship between BRAF^{V600E}, NF-κB and TIMP-1, we further silenced TIMP-1 gene in BCPAP cell line by using a specific siRNA. Silencing efficacy is shown in Fig. 9A. We next evaluate whether also TIMP-1 inhibition can affect invasion in siRNA treated BCPAP cells. So, as described above, after 24 hrs in a BioCoated MatrigelTM chamber, we showed that down-regulation of TIMP-1 gene decreased significantly BCPAP ability to invade (p=0.0002) (Fig. 9B and 9C).

Furthermore we showed that TIMP-1 silencing did not affect either BRAF^{V600E} expression or NF-κB activity (Fig. 9D and 9E) demonstrating that TIMP-1 protein is downstream to BRAF^{V600E} and NF-κB.

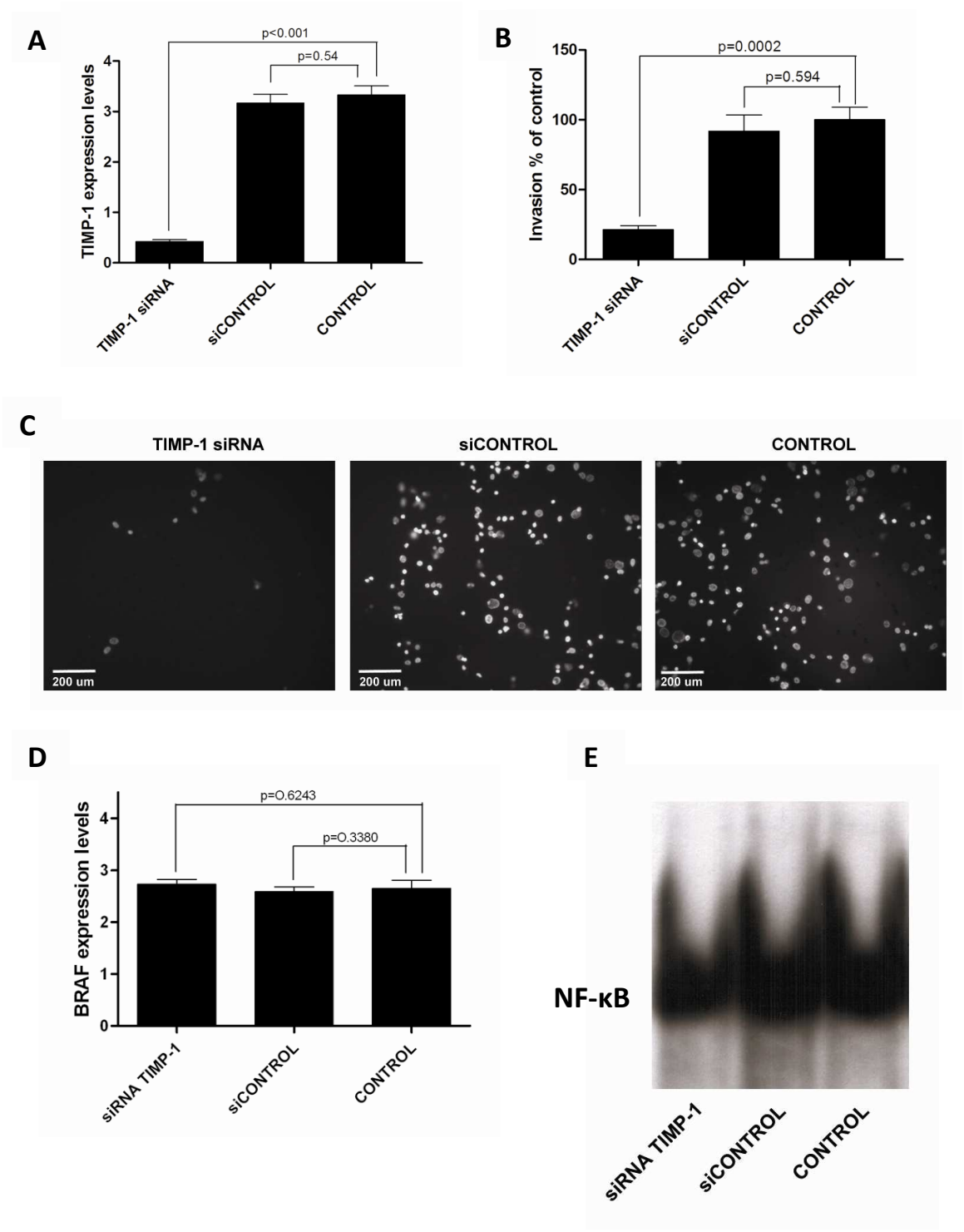

***Figure 9**. TIMP-1 silencing tumor invasion in BCPAP cell line and does not affect BRAF expression and NF-κB binding activity in BCPAP cell line. **(A)** qRT-PCR shows that specific TIMP-1 siRNA reduces TIMP-1 expression in comparison to untreated cells (p<0.001). Data are normalized against β-actin gene expression. **(B)** Invading cells are reduced after TIMP-1 silencing (left panel) in comparison to siCONTROL (central panel) and untreated cells (right panel). Scale bar 200 μm. **(C)** Quantification of cell invasion. Percentages of cell migration after TIMP-1 silencing considering control as 100%. Data are represented as mean ± SD of three experiments performed in triplicates. **(D)** qRT-PCR of BRAF expression after TIMP-1 siRNA treatment, scrambled siRNA (siCONTROL) and untreated cells (CONTROL). After 72 hrs TIMP-*

1 siRNA does not affect BRAF expression. ***(E)*** *NF-κB binding activity after TIMP-1 silencing is not affected. The analysis of NF-κB binding activity proves to be unaltered in BCPAP cells treated as well as in siCONTROL and untreated cells. Data are representative of at least three independent experiments.*

To investigate the relationship between NF-κB and TIMP-1, we treated BCPAP cells with dexamethasone, a generic inhibitor of the inflammatory pathway; parthenolide, a specific NF-κB inhibitor; and MG-132, a proteasome inhibitor blocking IκBα degradation (130, 131). We then evaluated TIMP-1 expression by qRT-PCR. Our results showed remarkable downregulation of TIMP-1 (Fig. 10A) which was confirmed by flow cytometry. In particular, TIMP-1 expression was consistently reduced after parthenolide (Fig 10 B-E).

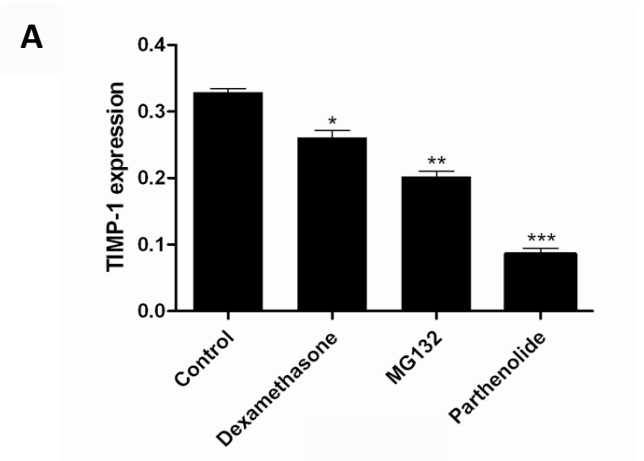

Figure 10*. TIMP-1 expression is significantly reduced after treatment with NF-κB inhibitors. BCPAP cells were stimulated for 24 hrs with 5 μM MG-132 (proteasome inhibitor), 50 nM dexamethasone 21-phosphate (nonspecific NF-κB inhibitor) and 10 μM parthenolide (specific NF-κB inhibitor) in the presence of monensin evaluated by means of qRT-PCR and flow cytometry.*

(A) *qRT-PCR shows a major reduction in TIMP-1 expression after treatment with all three drugs. This reduction is higher with parthenolide, which is a specific NF-κB inhibitor. * p<0.05; ** p<0.01; *** p<0.001.*

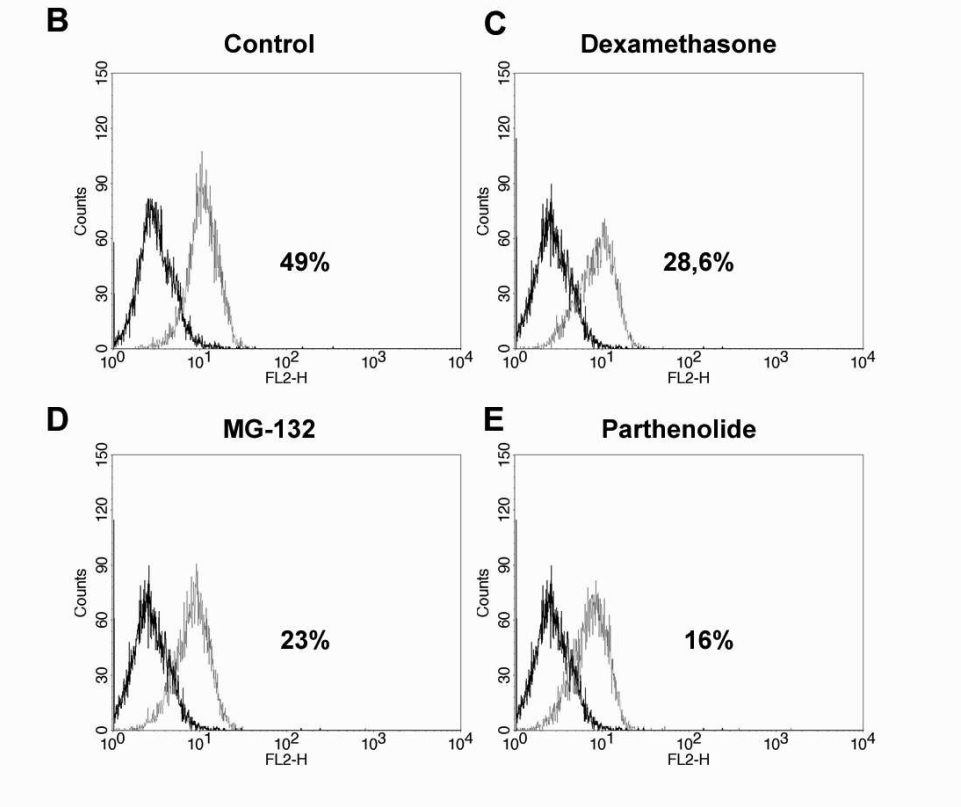

Figure 10 B–E. *Quantification of TIMP-1 expression by flow cytometry confirms the higher decrease after parthenolide. Data are representative of three independent experiments.*

Our data collectively show that a $BRAF^{V600E}$/NF-κB/TIMP-1/CD63 pathway exists in BCPAP cell line.

It has been demonstrated in colorectal and breast cancer that binding TIMP-1 with CD63 upregulates cell proliferation through Akt phosphorylation at Ser-473 (133). To clarify whether TIMP-1 activates Akt phosphorylation in PTC, we forced expression of TIMP-1 in BCPAP cell line by treatment with recombinant TIMP-1 at different concentrations (10-250 ng/ml) and time points (30 and 60 min). BrdU proliferation assay showed that TIMP-1 treated cells exhibit concentration-dependent proliferative activity in comparison to untreated cells, with higher values at 250 ng/ml (Fig. 11A). Indeed, treatment with 250 ng/ml TIMP-1 induced Akt phosphorylation already at 30 min (Fig. 11B).

We also treated BCPAP cell line with rTIMP-1 at 250 ng/ml for 24 hrs in a BioCoated MatrigelTM chamber and we showed that treated cells exhibit an increased invasion capability (p=0.0009) (Fig. 11C and D).

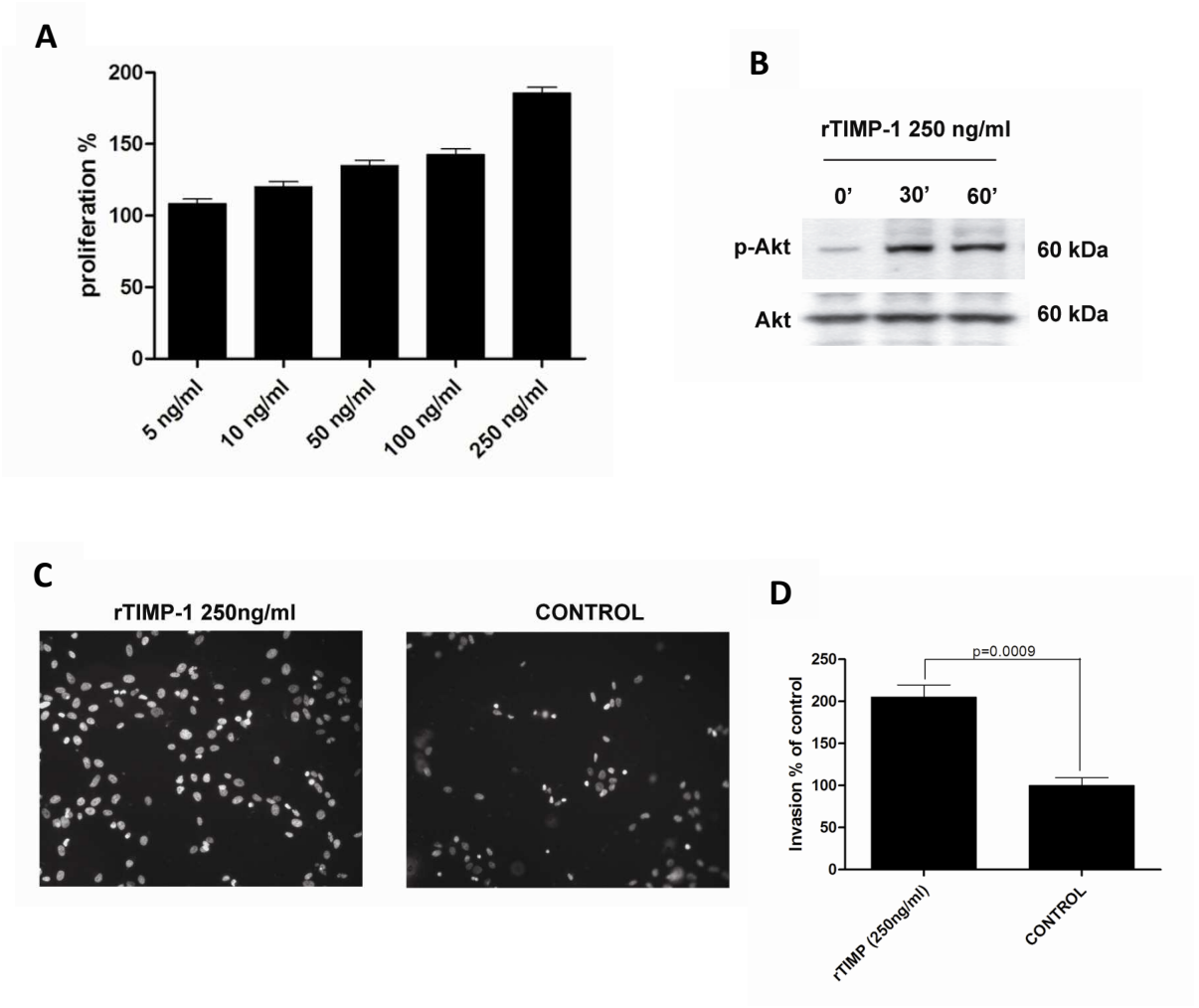

Figure 11*. Treatment of BCPAP cell line with rTIMP-1 increases cell proliferation, induces Akt phosphorylation and induces cell invasion.* ***(A)*** *BCPAP cells were incubated for 24 hrs with rTIMP-1 at different concentrations. The amount of newly synthesized DNA in proliferating cells measured by a BrdU incorporation assay increased directly to rTIMP-1 concentrations.* ***(B)*** *Cells were treated with rTIMP-1 (250 ng/ml) for 30 and 60 minutes. Western blot analysis was performed with Akt and p-Akt specific antibodies. The treatment already induced Akt phosphorylation after 30 minutes in comparison to untreated cells.* ***(C)*** *Invading cells are increased after rTIMP-1 treatment (left panel) in comparison to untreated cells (right panel). Scale bar 200 µm.* ***(D)*** *Quantification of cell invasion (p=0.0009).*

We then investigated the Akt-dependent proliferative activity of TIMP-1. To this end, we treated BCPAP cells with doxorubicin after addition of exogenous TIMP-1, silencing of TIMP-1 and/or BRAF. As expected, cell viability was significantly increased in TIMP-1 treated cells in a dose-dependent manner. By contrast, it was reduced after silencing with single or combined BRAF and TIMP-1 siRNA. This inhibition was not caspase 3-related (Fig. 12A).

These data collectively confirm TIMP-1 capacity to confer resistance to doxorubicin. To further assess targets of Akt which are involved in regulation of cell proliferation and apoptosis, we evaluated Bcl-xL and Bcl-2 expression in cells treated with 250 ng/ml recombinant TIMP-1. As expected, both anti-apoptotic molecules were hyper-expressed (Fig. 12B).

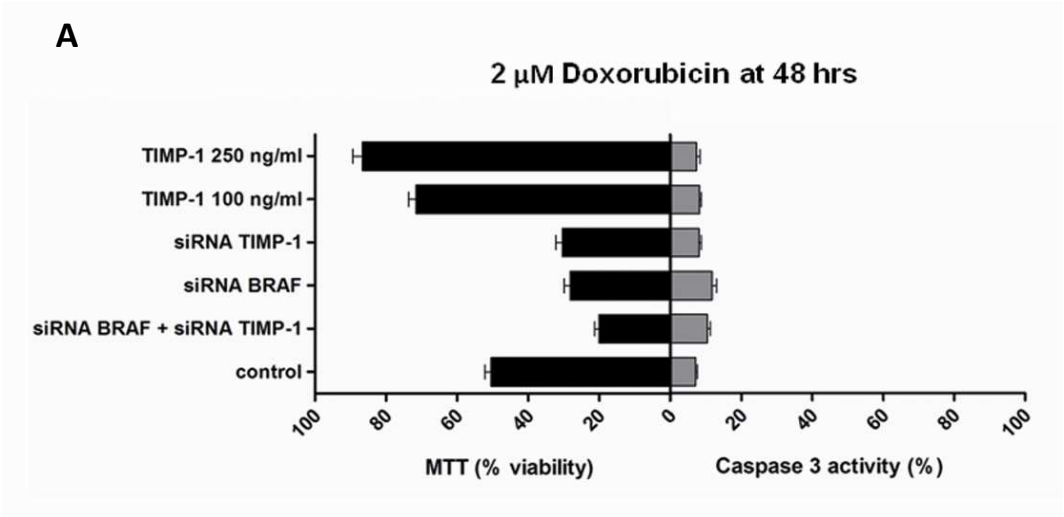

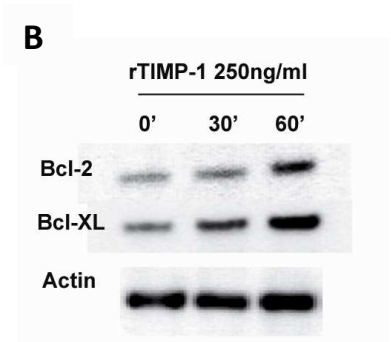

***Figure 12**. Treatment of BCPAP cell line with rTIMP-1 determines doxorubicin resistance and non-caspase-3 mediated anti-apoptotic activity. **(A)** BCPAP cell line were cultured for 48 hrs with 2 μM doxorubicin in the presence of 100 or 250 ng/ml rTIMP-1; 100 nM TIMP-1 siRNA; 100 nM BRAF siRNA; or TIMP-1 and BRAF siRNA combined. Cell viability (MTT) was reduced after TIMP-1 siRNA, BRAF siRNA and TIMP-1+BRAF siRNA, whereas it increased after rTIMP-1 addition. Caspase-3 activity was not affected by any*

*treatment**. (B)** Hyperexpression of Bcl-xL and Bcl-2 in BCPAP cells treated with 250 ng/ml rTIMP-1. Data are representative of three independent experiments.*

To confirm our data, we treated BCPAP cell line with a specific inhibitor of Akt1/2, and just after 4 hours of treatment, there was a significant reduction of the phosphorylated form of Akt (Fig. 13C). We also treated BCPAP cell line for 24 hrs in a BioCoated MatrigelTM chamber and we showed that treated cells have a reduced invasion capability ($p<0.0001$) (Fig. 13A and B). Furthermore, BrdU proliferation assay showed that the inhibition of Akt caused a reduced proliferative capability (Fig. 13D).

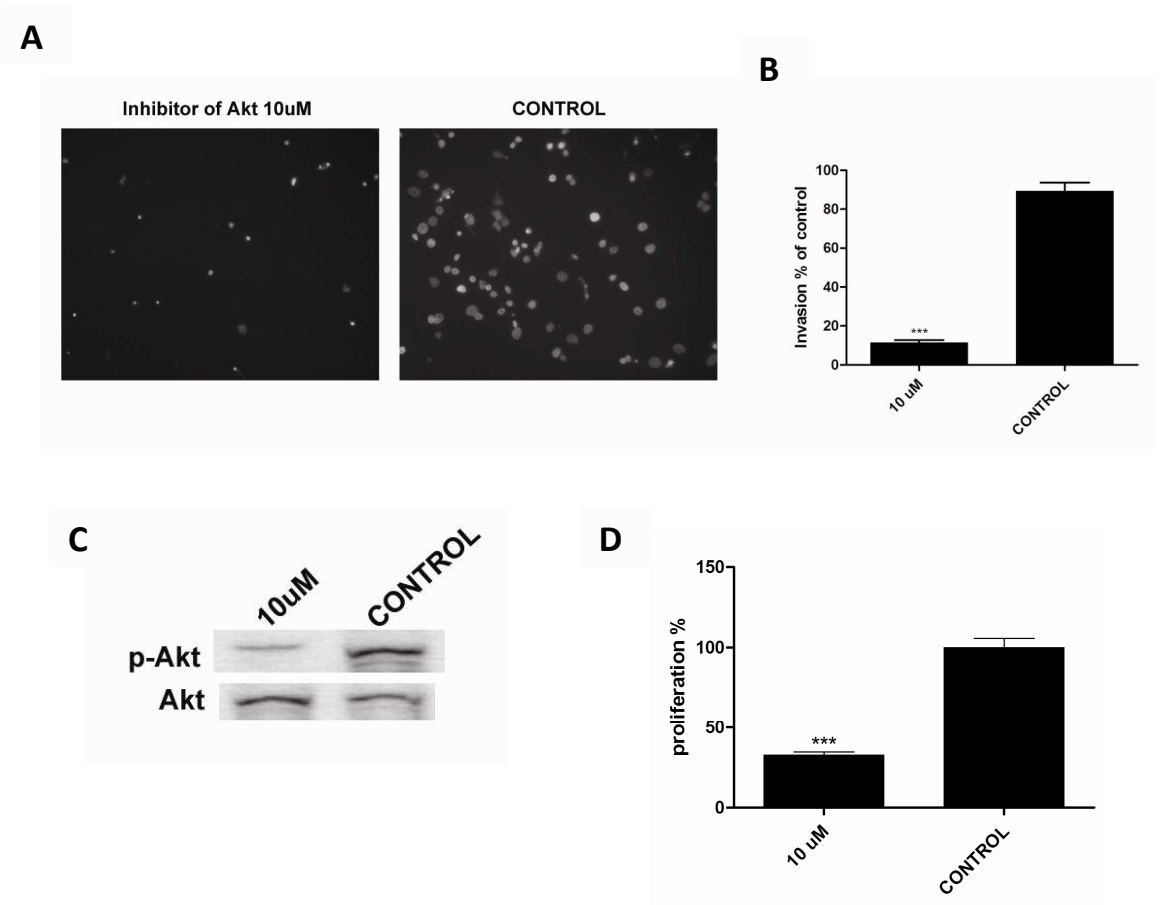

***Figure 13**. Akt1/2 inhibitor reduces cell invasion and cell proliferation capabilities. **(A)** BCPAP cell line was cultured for 24 hrs with 10 uM inhibitor of Akt1/2 in a BioCoated MatrigelTM chamber. Invading cells are decreased after treatment (left panel) in comparison to untreated cells (right panel). Scale bar 200 µm. **(B)** Quantification of cell invasion ($p<0.0001$). **(C)** Cells were treated with specific inhibitor of Akt1/2 (10uM) for 1 hour. Western blot analysis was performed with Akt and p-Akt specific antibodies. The treatment reduced Akt phosphorylation in*

comparison to untreated cells. ***(D)*** *BCPAP cells were incubated for 24 hrs with 10 uM inhibitor of Akt1/2. The amount of newly synthesized DNA in proliferating cells measured by a BrdU incorporation assay decreased.*

DISCUSSION

Our study demonstrates the existence of a trilogy involving $BRAF^{V600E}$, NF-κB and TIMP-1 in *ex vivo* PTCs.

We provided the proof of the principle by using an *in vitro* model which confirmed that $BRAF^{V600E}$ activates NF-κB and subsequently increases TIMP-1 expression, which in turn binds CD63 leading to Akt phosphorylation. This pathway eventually results in increased proliferation and invasiveness, inhibiting apoptosis and conferring resistance to doxorubicin.

We found TIMP-1 hyperexpression in $BRAF^{V600E}$-mutated PTCs. TIMP-1 is known as a specific inhibitor of MMP-9. Recently it has been proposed that TIMP-1 possess functions independent of MMP-9 inhibition. These mechanisms may be involved in extrathyroidal invasion and metastasis of PTCs harboring $BRAF^{V600E}$. Accordingly, conditional expression of BRAF was associated with markedly increased invasion of Matrigel compared with cells expressing RET/PTC3 (131). Here we confirm increased MMP-9 activity in PTC nodules, along with TIMP-1 hyperexpression. The role played by $BRAF^{V600E}$ on cell invasion was proved on BCPAP cells after silencing along with remarkable inhibition of cell invasiveness.

We also found hyperactivation of the NF-κB system, which we propose could be the link between $BRAF^{V600E}$ mutation and TIMP-1 hyper-expression, as Palona et al has described (55). Palona, in fact, has demonstrated that the degradation of IκB-α, a cytoplasmic inhibitor of NF-κB, started shortly after a sufficient accumulation of $BRAF^{V600E}$ protein, resulting in the activation of NF-κB signaling. Furthermore a specific NF-κB inhibitor, DHMEQ, efficiently blocked $BRAF^{V600E}$-induced NF-κB activation. Interestingly, however, this activation was independent of MEK-ERK pathway. This is consistent with a previous report showing that the constitutive active mutant of MEK failed to induce NF-κB-

dependent gene expression in NIH3T3 cells, whereas RASV12 or CRAFBXB (both are also constitutive active mutants) were capable of it (135).

Although our study does not describe through which mechanisms $BRAF^{V600E}$ mutation activates NF-κB, we accordingly to Palona showed that silencing of $BRAF^{V600E}$ resulted in decreased NF-κB and TIMP-1 expression. This observation suggests that $BRAF^{V600E}$ mutation is an upstream event that activates NF-κB.

Figure 14 summarizes the proposed molecular mechanism for the interaction of $BRAF^{V600E}$, NF-κB and TIMP-1.

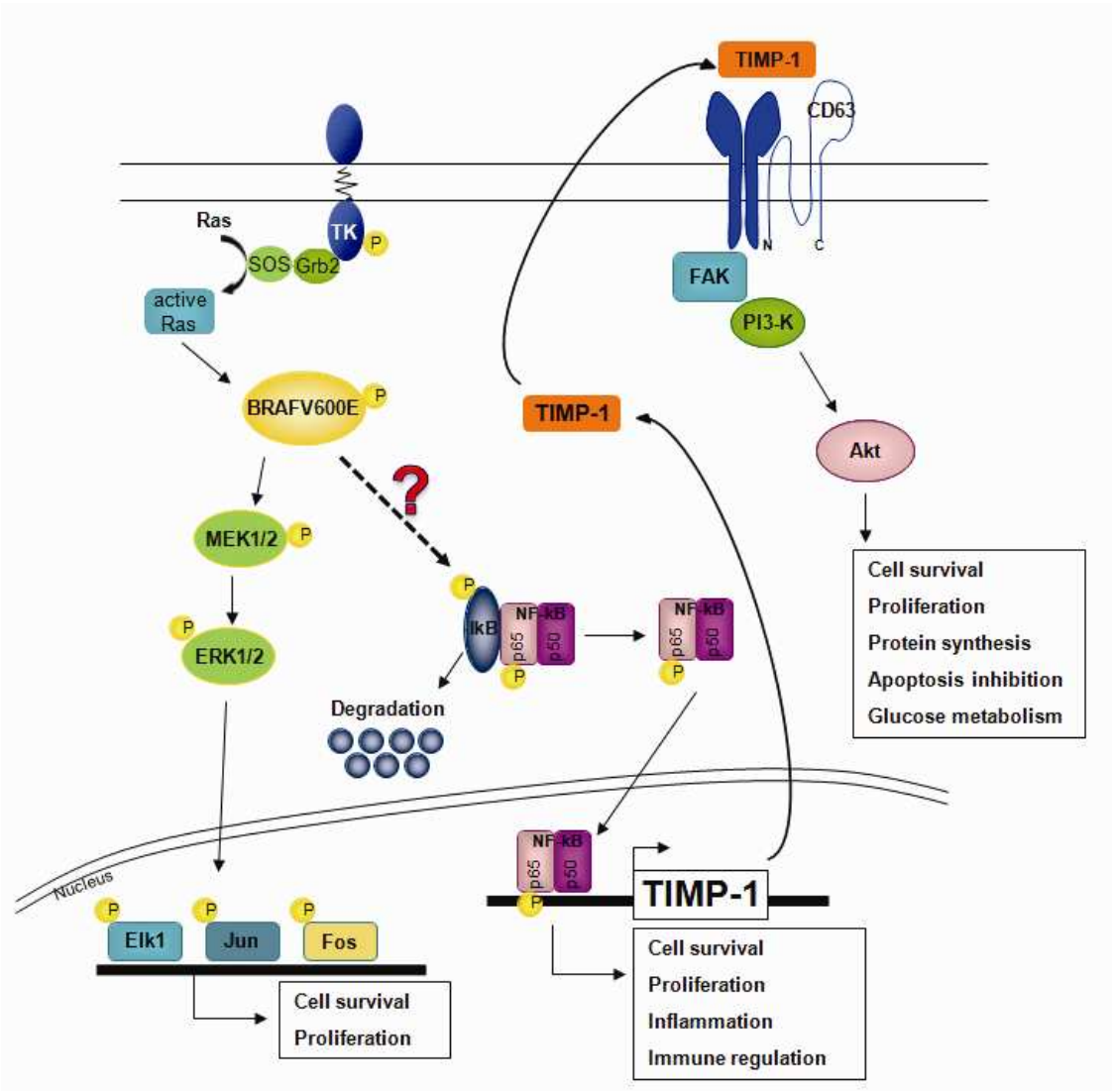

***Figure 14**. Molecular mechanism for the interaction of $BRAF^{V600E}$, NF-κB and TIMP-1. Left panel: BRAF conventional pathway. Right: proposed $BRAF^{V600E}$ pathway. $BRAF^{V600E}$ activates*

NF-κB and subsequently increases TIMP-1 expression, which in turn binds CD63 leading to Akt phosphorylation. Dashed arrow indicates molecular mechanism through BRAF^{V600E} activates IκB degradation described by Palona et al (55).

Conversely, silencing of TIMP-1 did not affect either BRAF^{V600E} or NF-κB, confirming TIMP-1 is the downstream factor of the trilogy. The link between these two players is NF-κB, as demonstrated by the decrease in TIMP-1 expression when NF-κB inhibitors were used.

We also identified one of the possible MMP-9-independent molecular mechanisms by which TIMP-1 exerts its biological activity on cell proliferation. TIMP-1 binds its receptor CD63 on cell surface membrane and activates the Akt signaling pathway trough PI3K. Akt then exerts its effects in the cell by phosphorylating a variety of downstream substrates, all resulting in anti-apoptotic or pro-proliferative effects (84, 135).

CD63^{+} cells were found in *ex vivo* PTCs and in BCPAP. Addition of recombinant TIMP-1 protein in our *in vitro* model resulted in enhanced Akt phosphorylation and activation that leads to increased proliferation. Furthermore, recombinant TMP-1 enhanced matrigel invasion capability and increases Bcl-xL and Bcl-2 expression via Akt, confirming the crucial involvement of the PI3-kinase pathway in TIMP-1 signaling (107). These results are consistent with the anti-apoptotic activity of TIMP-1 mediated by CD63 binding (84).

Conversely, Akt specific inhibition caused reduced proliferation and invasion capability, demonstrating that the TIMP-1, the final step of the “trilogy” we have described, regulates proliferation and invasion capabilities trough Akt pathway.

In conclusion, we describe the existence of a link among three well-recognized factors involved in PTC tumorigenesis. These findings suggest that targeting such trilogy might be useful for the treatment of PTC.

References

1. Nillson M. Iodide handling by the thyroid epithelial cell. Exp Clin Endocrinol Diabetes 2001;109(1):13–7.

2. Xing M. Recent Advances in Molecular Biology of Thyroid Cancer and Their Clinical Implications. Otolaryngol Clin North Am. 2008 December ; 41(6): 1135–1146.

3. Davies L, Welch HG. Increasing incidence of thyroid cancer in the United States, 1973-2002. JAMA 2006;295(18):2164–67.

4. Schlumberger MJ. Papillary and follicular thyroid carcinoma. N Engl J Med 1998; 338: 297-306.

5. NCI data at: http://www.cancer.gov/cancertopics/types/thyroid.

6. Pellegriti G, De Vathaire F, Scollo C, Attard M, Giordano C, Arena S, Dardanoni G, Frasca F, Malandrino P, Vermiglio F, Previtera DM, D'Azzò G, Trimarchi F, Vigneri R. Papillary thyroid cancer incidence in the volcanic area of Sicily. J Natl Cancer Inst. 2009 Nov 18;101(22):1575-83.

7. Leenhardt L, Grosclaude P, Cherie-Challine L. Increased incidence of thyroid carcinoma in France: a true epidemic or thyroid nodule management effects? report from the French thyroid cancer committee. Thyroid 2004;14(12):1056–60.

8. Hundahl SA, Fleming ID, Fremgen AM, et al. A National Cancer Data Base report on 53,856 cases of thyroid carcinoma treated in the U.S., 1985-1995. Cancer 1998;83(12):2638–48.

9. Cornett WR, Sharma AK, Day TA, et al. Anaplastic thyroid carcinoma: an overview. Curr Oncol Rep 2007;9(2):152–8.

10. Hundahl SA, Fleming ID, Fremgen AM, Menck HR. A National Cancer Data Base report on 53,856 cases of thyroid carcinoma treated in U.S., 1985-1995. Cancer 1998; 83: 2638-2648.

11. Cooper DS, Doherty GM, Haugen BR, et al. Management guidelines for patients with thyroid nodules and differentiated thyroid cancer. Thyroid 2006; 16: 109-142.

12. Kohno M, Pouyssegur J. Targeting the ERK signaling pathway in cancer therapy. Ann Med 2006;38 (3):200–11.

13. Fagin JA 2002 Minireview: branded from the start-distinct oncogenic initiating events may determine tumor fate in the thyroid. Molecular Endocrinology 16 903–911.

14. Nikiforov YE 2002 RET/PTC rearrangement in thyroid tumors. Endocrine Pathology 13 3–16.

15. McIver B, Grebe SK & Eberhardt NL 2004 The PAX8/ PPARgamma fusion oncogene as a potential therapeutic target in follicular thyroid carcinoma. Current Drug Targets. Immune, Endocrine and Metabolic Disorders 4 221–234.

16. Davies H, Bignell GR, Cox C, et al. Mutations of the BRAF gene in human cancer. Nature 2002;417 (6892):949–54.

17. Mercer KE, Pritchard CA. Raf proteins and cancer: B-Raf is identified as a mutational target. Biochimica et Biophysica Acta 2003;1653(1):25–40.

18. Dhillon AS & Kolch W 2004 Oncogenic B-Raf mutations: crystal clear at last. Cancer Cell 5 303–304.

19. Xing M. BRAF mutation in thyroid cancer. Endocrine-Related Cancer (2005) 12 245–262.

20. Garnett MJ, Marais R. Guilty as charged: B-RAF is a human oncogene. Cancer Cell 2004;6(4):313–9.

21. Xing M. BRAF mutation in papillary thyroid cancer: pathogenic role, molecular bases, and clinical implications. Endocr Rev 2007;28(7):742–62.

22. Trovisco V, Vieira de Castro I, Soares P, et al. BRAF mutations are associated with some histological types of papillary thyroid carcinoma. J Pathol 2004;202(2):247–51.

23. Ciampi R, Knauf JA, Kerler R, et al. Oncogenic AKAP9-BRAF fusion is a novel mechanism of MAPK pathway activation in thyroid cancer. J Clin Invest 2005;115(1):94–101.

24. Hou P, Liu D, Xing M. Functional characterization of the T1799-1801del and A1799-1816ins BRAF mutations in papillary thyroid cancer. Cell Cycle 2007;6(3):377–9.

25. Moretti S, Macchiarulo A, De Falco V, et al. Biochemical and molecular characterization of the novel BRAF(V599Ins) mutation detected in a classic papillary thyroid carcinoma. Oncogene 2006;25(30): 4235–40.

26. Xing M. The T1799A BRAF mutation is not a germline mutation in familial nonmedullary thyroid cancer. Clin Endocrinol 2005;63(3):263–6.

27. Knauf JA, Ma X, Smith EP, et al. Targeted expression of BRAFV600E in thyroid cells of transgenic mice results in papillary thyroid cancers that undergo dedifferentiation. Cancer Res 2005;65(10): 4238–45.

28. Liu D, Liu Z, Condouris S, et al. BRAF V600E maintains proliferation, transformation and tumorigenicity of BRAF mutant papillary thyroid cancer cells. J Clin Endocrinol Metab 2007;92(6): 2264–71.

29. Abrosimov A, Saenko V, Rogounovitch T, Namba H, Lushnikov E, Mitsutake N, Yamashita S 2007 Different structural components of conventional papillary thyroid carcinoma display mostly identical BRAF status. Int J Cancer 120:196–200

30. Adeniran AJ, Zhu Z, Gandhi M, Steward DL, Fidler JP, Giordano TJ, Biddinger PW, Nikiforov YE 2006 Correlation between genetic alterations and microscopic features, clinical manifestations, and prognostic characteristics of thyroid papill ary carcinomas. Am JSurg Pathol 30:216–222

31. Riesco-Eizaguirre G, Gutierrez-Martinez P, Garcia-Cabezas MA, Nistal M, Santisteban P 2006 The oncogene BRAF V600E is associated with a high risk of recurrence and

less differentiated papillary thyroid carcinoma due to the impairment of Na+/I- targeting to the membrane. Endocr Relat Cancer 13:257–269

32. Frasca F, Nucera C, Belfiore A, Piero G, Attard M, Stella M, Pellegriti G, Giordano C, Trimarchi F, Vigneri R 2006 BRAF T1799A mutation in thyroid cancer predicts progressive disease. Program of the 88th Annual Meeting of The Endocrine Society, June 24–27, 2006, Boston, MA.

33. Kebebew E, Weng J, Bauer J, Ranvier G, Clark OH, Duh QY, Shibru D, Bastian B, GriffinA2007 The prevalence and prognostic value of BRAF mutation in thyroid cancer. Ann Surg 246:466–471

34. Rodolico V, Cabibi D, Pizzolanti G, Richiusa P, Gebbia N, Martorana A, Russo A, Amato MC, Galluzzo A, Giordano C 2007 BRAF(V600E) mutation and p27(kip1) expression in papillary carcinomas of the thyroid ≤1 cm and their paired lymph node metastases. Cancer 110:1218–1226.

35. Xing M, Westra WH, Tufano RP, et al. BRAF mutation predicts a poorer clinical prognosis for papillary thyroid cancer. J Clin Endocrinol Metab 2005;90(12):6373–9.

36. Liu D, Hu S, Hou P, et al. Suppression of BRAF/MEK/MAP kinase pathway restores expression of iodide-metabolizing genes in thyroid cells expressing the V600E BRAF mutant. Clin Cancer Res 2007;13(4):1341–49.

37. Durante C, Puxeddu E, Ferretti E, et al. BRAF mutations in papillary thyroid carcinomas inhibit genes involved in iodine metabolism. J Clin Endocrinol Metab 2007;92(7):2840–43.

38. Romei C, Ciampi R, Faviana P, et al. BRAFV600E mutation, but not RET/PTC rearrangements, is correlated with a lower expression of both thyroperoxidase and sodium iodide symporter genes in papillary thyroid cancer. Endocr Relat Cancer 2008;15(2):511–20.

39. Di Cristofaro J, Silvy M, Lanteaume A, et al. Expression of TPO mRNA in thyroid tumors: quantitative PCR analysis and correlation with alterations of ret, Braf, ras and pax8 genes. Endocr Relat Cancer 2006;13(2):485–95.

40. Mian C, Barollo S, Pennelli G, et al. Molecular characteristics in papillary thyroid cancers (PTCs) with no 131I uptake. Clin Endocrinol (Oxf) 2008;68(1):108–16.

41. Basseres DS, Baldwin AS. Nuclear factor-kappaB and inhibitor of kappaB kinase pathways in oncogenic initiation and progression. Oncogene 2006;25:6817–30.

42. Jost PJ, Ruland J. Aberrant NF-kappaB signaling in lymphoma: mechanisms, consequences, and therapeutic implications. Blood 2007;109:2700–7.

43. Dutta J, Fan Y, Gupta N, Fan G, Gelinas C. Current insights into the regulation of programmed cell death by NF NF-kappaB. Oncogene 2006;25:6800–16.

44. Baud V, Karin M. Is NF-κB a good target for cancer therapy? Hopes and pitfalls. Is NF-κB a good target for cancer therapy? Hopes and pitfalls.

45. Ghosh S, May MJ, Kopp EB. NF-kappa B and Rel proteins: evolutionarily conserved mediators of immune responses. Annu Rev Immunol 1998;16:225–60.

46. Ghosh S, Karin M. Missing pieces in the NF-kappaB puzzle. Cell 2002;109 (Suppl):S81–96.

47. Bonizzi G, Karin M. The two NF-kappaB activation pathways and their role in innate and adaptive immunity. Trends Immunol 2004;25:280–8.

48. Claudio E, Brown K, Park S, Wang H, Siebenlist U. BAFF-induced NEMO-independent processing of NF-kappa B2 in maturing B cells. Nat Immunol 2002;3:958–65.

49. Dejardin E. The alternative NF-kappaB pathway from biochemistry to biology: pitfalls and promises for future drug development. Biochem Pharmacol 2006;72:1161–79.

50. Pomerantz JL, Baltimore D. Two pathways to NF-kappaB. Mol Cell 2002;10:693–5.

51. Shattuck-Brandt RL, Richmond A. Enhanced degradation of I-kappaB alpha contributes to endogenous activation of NF-κB in Hs294T melanoma cells. Cancer Res 1997; 57: 3032-3039.

52. Sweeney C, Li L, Shanmugam R, et al. Nuclear factor-kappaB is constitutively activated in prostate cancer in vitro and is overexpressed in prostatic intraepithelial neoplasia and adenocarcinoma of the prostate. Clin Cancer Res 2004; 10: 5501-5507.

53. Visconti R, Cerutti J, Battista S, et al. Expression of the neoplastic phenotype by human thyroid carcinoma cell lines requires NF-κB p65 protein expression. Oncogene 1997; 15: 1987-1994.

54. Pacifico F, Leonardi A. Role of NF-kappaB in thyroid cancer. Mol Cell Endocrinol 2010; 321: 29-35.

55. Palona I, Namba H, Mitsutake N, et al. $BRAF^{V600E}$ promotes invasiveness of thyroid cancer cells through nuclear factor kB activation. Endocrinology 2006; 147: 5699-5707.

56. Karin M. Nuclear factor-kB in cancer development and progression. Nature 2006; 441: 431-436.

57. Gilmore TD. Multiple mutations contribute to the oncogenicity of the retroviral oncoprotein v-Rel. Oncogene 1999;18:6925-37.

58. Morin CI, Huot J. Recent advances in stress signaling in cancer. Cancer Res 2004;64:1893-8.

59. Pacifico F, Leonardi A. NF-kappaB in solid tumors. Biochem Pharmacol. 2006 Oct 30;72(9):1142-52.

60. Kucharczak J, Simmons MJ, Fan Y, Gelinas C. To be, or not to be: NF-κB is the answer — role of Rel/NF-κB in the regulation of apoptosis. Oncogene 2003;22:8961-82

61. Romieu-Mourez R, Kim DW, Shin SM, Demicco EG, Landesman- Bollag E, Seldin DC, et al. Mouse mammary tumor virus c-rel transgenic mice develop mammary tumors. Mol Cell Biol 2003;23:5738-54.

62. Wang CY, Cusack JC, Jr., Liu R, Baldwin AS, Jr. Control of inducible chemoresistance: enhanced anti-tumor therapy through increased apoptosis by inhibition of NF-κB. Nature Med 1999;5:412-7.

63. Bargou RC, Emmerich F, Krappmann D, Bommert K, Mapara MY, Arnold W, et al. Constitutive nuclear factor-κB-RelA activation is required for proliferation and survival of Hodgkin's disease tumor cells. J Clin Invest 1997;100:2961-9.

64. Namba H, Saenko V, Yamashita S. Nuclear factor-kB in thyroid carcinogenesis and progression: a novel therapeutic target for advanced thyroid cancer. Arq Bras Endocrinol Metabol. 2007 Jul;51(5):843-51.

65. Pikarsky E, Porat RM, Stein I, Abramovitch R, Amit S, Kasem S, et al. NF-κB functions as a tumour promoter in inflammation-associated cancer. Nature 2004;431:461-6.

66. Pacifico F, Mauro C, Barone C, Crescenzi E, Mellone S, Monaco M, et al. Oncogenic and anti-apoptotic activity of NF-κB in human thyroid carcinomas. J Biol Chem 2004;279:54610-9.

67. Mitsiades CS, Kotoula V, Poulaki V, Sozopoulos E, Negri J, Charalambous E, et al. Epidermal growth factor receptor as a therapeutic target in human thyroid carcinoma: mutational and functional analysis. J Clin Endocrinol Metab 2006;91:3662-6.

68. Kimura ET, Nikiforova MN, Zhu Z, Knauf JA, Nikiforov YE, Fagin JA. High prevalence of BRAF mutations in thyroid cancer: genetic evidence for constitutive activation of the RET/PTC-RAS-BRAF signaling pathway in papillary thyroid carcinoma. Cancer Res 2003;63:1454-7.

69. Tuyt LM, Dokter WH, Birkenkamp K, Koopmans SB, Lummen C, Kruijer W, et al. Extracellular-regulated kinase 1/2, Jun Nterminal kinase, and c-Jun are involved in NF-κB-dependent IL-6 expression in human monocytes. J Immunol 1999;162:4893-902.

70. Ludwig L, Kessler H, Wagner M, Hoang-Vu C, Dralle H, Adler G, et al. Nuclear factor-κB is constitutively active in C-cell carcinoma and required for RET-induced transformation. Cancer Res 2001;61:4526-35.

71. Johansson N, Ala-aho R, Uitto V, Grénman R, Fuseing NE, Lòpez-òtin C, Kähari VM. Expression of collagenase-3 (MMP-13) and collagenase-1 (MMP-1) by transformed keratinocytes is dependent on the activity of p38 mitogen-activated protein kinase, J Cell Sci, 2000,113 Pt 2:227–235.

72. Amălinei C, Căruntu ID, Giuşcă SE, Bălan RA. Matrix metalloproteinases involvement in pathologic conditions. Rom J Morphol Embryol. 2010;51(2):215-28.

73. Visse R, Nagase H: Matrix metalloproteinases and tissue inhibitors of metalloproteinases: structure, function, and biochemistry. Circ Res 2003, 92:827-39.

74. Chaudhary AK, Singh M, Bharti AC, Asotra K, Sundaras S, Mehrotra R. Genetic polymorphisms of matrix metalloproteinases and their inhibitors in potentially malignant and malignant lesions of the head and neck. Journal of Biomedical Science 2010, 17:10.

75. Sternlicht MD, Werb Z: How matrix metalloproteinases regulate cell behavior. Annu Rev Cell Dev Bio 2001, 17:463-16.

76. Westermarck J, Kahari V-M: Regulation of matrix metalloproteinase expression in tumour invasion. FASE 1999, 13:781-92.

77. Brew K, Dinakapandian D, Nagase H: Tissue inhibitors of metalloproteinases: evolution, structure and function. Biochim Biophys Acta 2000, 1477:267-83.

78. Gohji K, Fujimoto N, Hara I, Fujii A, Gotoh A, Okada H, Arakawa S, Kitazawa S, Miyake H, Kamidono S, Nakajima M 1998 Serum matrix metalloproteinases-2 and hits density

in men with prostate cancer as a new predictor of disease extension. Int J Cancer 79:96–101.

79. Ahmad A, Hanby A, Dublin E, Poulsom R, Smith P, Barnes D, Rubens R, Anglard P, Hart I 1998 Stromelysin 3: An independent prognostic factor for relapse-free survival in node-positive breast cancer and demonstration of novel breast carcinoma cell expression. J Am J Pathol 152:721–728.

80. Baldini E, Toller M, Graziano FM, Russo FP, Pepe M, Biordi L, Marchioni E, Curcio F, Ulisse S, Ambesi-Impiombato FS, D'Armiento M. Expression of matrix metalloproteinases and their specific inhibitors in normal and different human thyroid tumor cell lines. Thyroid. 2004 Nov;14(11):881-8.

81. Jaworski DM, Soloway P, Caterina J, Falls WA. Tissue inhibitor of metalloproteinase-2(TIMP-2)- deficient mice display motor deficits. Journal of Neurobiology 2006;66:82–94.

82. Apte SS, Mattei MG, Olsen BR: Cloning of the cDNA encoding human tissue inhibitor of metalloproteinases-3 (TIMP-3) and mapping of the TIMP3 gene to chromosome 22. Genomics 1994, 19:86-90. 69.

83. Olson TM, Hirohata S, Ye J, Leco K, Seldin MF, Apte SS: Cloning of the human tissue inhibitor of metalloproteinase-4 gene (TIMP4) and localization of the TIMP-4 and Timp4 genes to human chromosome 3p25 and mouse chromosome 6, respectively. Genomics 1998, 51:148-51.

84. Stetler-Stevenson WG. Tissue inhibitors of metalloproteinases in cell signaling: metalloproteinase-independent biological activities. Sci. Signal 2008; 1(27) re6.

85. Tuuttila A, Morgunova E, Bergmann U, Lindqvist Y, Maskos K, Fernandez-Catalan C, Bode W, Tryggvason K, Schneider G. Three-dimensional structure of human tissue inhibitor of metalloproteinases-2 at 2.1 A resolution. Journal of Molecular Biology 1998;284:1133–1140.

86. Yu WH, Yu S, Meng Q, Brew K, Woessner JF Jr. TIMP-3 binds to sulfated glycosaminoglycans of the extracellular matrix. Journal of Biological Chemistry 2000;275:31226–31232.

87. Greene J, Wang M, Liu YE, Raymond LA, Rosen C, Shi YE: Molecular cloning and characterization of human tissue inhibitor of metalloproteinase 4. J Biol Chem 1996, 271(48):30375-30380.

88. Melendez-Zajgla J, Del Pozo L, Ceballos G, Maldonado V. Tissue inhibitor of metalloproteinases-4. The road less traveled. Mol Cancer. 2008 Nov 21;7:85.

89. Brew K, Dinakarpandian D, Nagase H: Tissue inhibitors of metalloproteinases: evolution, structure and function. Biochim Biophys Acta 2000, 1477:1-2.

90. Derry JM, Barnard PJ: Physical linkage of the A-raf-1, properdin, synapsin I, and TIMP genes on the human and mouse X chromosomes. Genomics 1992, 12(4):632-638.

91. Clark IM, Swingler TE, Sampieri CL, Edwards DR. The regulation of matrix metalloproteinases and their inhibitors. International Journal of Biochemistry & Cell Biology. 2008doi:10.1016/jbiocel. 2007.12.006.

92. Barasch J, Yang J, Qiao JZ, Tempst P, Erdjument-Bromage H, Leung W, Oliver JA. Tissue inhibitor of metalloproteinase-2 stimulates mesenchymal growth and regulates epithelial branching during morphogenesis of the rat metanephros. Journal of Clinical Investigation 1999;103:1299–1307.

93. Docherty AJ, Lyons A, Smith BJ, Wright EM, Stephens PE, Harris TJ, Murphy G, Reynolds JJ. Sequence of human tissue inhibitor of metalloproteinases and its identity to erythroid-potentiating activity. Nature. 1985 Nov 7-13;318(6041):66-9.

94. Williamson RA, Marston FA, Angal S, Koklitis P, Panico M, Morris HR, Carne AF, Smith BJ, Harris TJ, Freedman RB. Disulphide bond assignment in human tissue inhibitor of metalloproteinases (TIMP). Biochem J.1990 Jun 1;268(2):267-74.

95. Murphy G, Houbrechts A, Cockett MI, Williamson RA, O'Shea M, Docherty AJ. The N-terminal domain of tissue inhibitor of metalloproteinases retains metalloproteinase inhibitory activity. Biochemistry. 1991 Aug 20;30(33):8097-102. Erratum in: Biochemistry 1991 Oct 22;30(42):10362.

96. Dean G, Young DA, Edwards DR, Clark IM. The human tissue inhibitor of metalloproteinases (TIMP)-1 gene contains repressive elements within the promoter and intron 1. Journal of Biological Chemistry 2000;275:32664–32671.

97. Kopitz C, Gerg M, Bandapalli OR, Ister D, Pennington CJ, Hauser S, Flechsig C, Krell HW, Antolovic D, Brew K, Nagase H, Stangl M, von Weyhern CW, Brucher BL, Brand K, Coussens LM, Edwards DR, Kruger A. Tissue inhibitor of metalloproteinases-1 promotes liver metastasis by induction of hepatocyte growth factor signaling. Cancer Research 2007;67:8615–8623.

98. Mohammed FF, Pennington CJ, Kassiri Z, Rubin JS, Soloway PD, Ruther U, Edwards DR, Khokha R. Metalloproteinase inhibitor TIMP-1 affects hepatocyte cell cycle via HGF activation in murine liver regeneration. Hepatology 2005;41:857–867.

99. Martin DC, Fowlkes JL, Babic B, Khokha R. Insulin-like growth factor II signaling in neoplastic proliferation is blocked by transgenic expression of the metalloproteinase inhibitor TIMP-1. Journal of Cell Biology 1999;146:881–892.

100. Griffith OL, Melck A, Jones SJM, Wiseman SM. Meta-Analysis and Meta-Review of thyroid cancer gene expression profiling studies identifies important diagnostic biomarkers. J. Clin. Oncol 2006; 24: 5043-5051.

101. Khokha R, Waterhouse P, Yagel S, Lala PK, Overall CM, Norton G, Denhardt DT. Antisense RNAinduced reduction in murine TIMP levels confers oncogenicity on Swiss 3T3 cells. Science 1989;243:947–950.

102. Montgomery AM, Mueller BM, Reisfeld RA, Taylor SM, DeClerck YA. Effect of tissue inhibitor of the matrix metalloproteinases-2 expression on the growth and spontaneous metastasis of a human melanoma cell line. Cancer Research 1994;54:5467–5473.

103. Egeblad M, Werb Z. New functions for the matrix metalloproteinases in cancer progression. Nature Reviews Cancer 2002;2:161–174.

104. Corcoran ML, Stetler-Stevenson WG. Tissue inhibitor of metalloproteinase-2 stimulates fibroblast proliferation via a cAMP-dependent mechanism. Journal of Biological Chemistry 1995;270:13453– 13459.

105. Yamashita K, Suzuki M, Iwata H, Koike T, Hamaguchi M, Shinagawa A, Noguchi T, Hayakawa T. Tyrosine phosphorylation is crucial for growth signaling by tissue inhibitors of metalloproteinases (TIMP-1 and TIMP-2). FEBS Letters 1996;396:103–107.

106. Wang T, Yamashita K, Iwata K, Hayakawa T. Both tissue inhibitors of metalloproteinases-1 (TIMP-1) and TIMP-2 activate Ras but through different pathways. Biochemical & Biophysical Research Communications 2002;296:201–205.

107. Guedez L, Stetler-Stevenson WG, Wolff L, Wang J, Fukushima P, Mansoor A, Stetler-Stevenson M. In vitro suppression of programmed cell death of B cells by tissue inhibitor of metalloproteinases-1. Journal of Clinical Investigation 1998;102:2002–2010.

108. Li G, Fridman R, Kim HR. Tissue inhibitor of metalloproteinase-1 inhibits apoptosis of human breast epithelial cells. Cancer Research 1999;59:6267–6275.

109. Zhao WQ, Li H, Yamashita K, Guo XK, Hoshino T, Yoshida S, Shinya T, Hayakawa T. Cell cycleassociated accumulation of tissue inhibitor of metalloproteinases-1 (TIMP-1) in the nuclei of human gingival fibroblasts. Journal of Cell Science 1998;111:1147–1153.

110. Jung KK, Liu XW, Chirco R, Fridman R, Kim HR. Identification of CD63 as a tissue inhibitor of metalloproteinase-1 interacting cell surface protein. EMBO J. 2006 Sep 6;25(17):3934-42. Epub 2006 Aug 17

111. Berditchevski F, Zutter MM, Hemler ME (1996) Characterization of novel complexes on the cell surface between integrins and proteins with 4 transmembrane domains (TM4 proteins). Mol Biol Cell 7: 193–207.

112. Yunta M, Lazo PA (2003) Tetraspanin proteins as organisers of membrane microdomains and signalling complexes. Cell Signal 15: 559–564.

113. Hildreth JE, Derr D, Azorsa DO (1991) Characterization of a novel self-associating Mr 40,000 platelet glycoprotein. Blood 77: 121–132.

114. Pfistershammer K, Majdic O, Stockl J, Zlabinger G, Kirchberger S, Steinberger P, KnappW(2004) CD63 as an activation-linked Tcell costimulatory element. J Immunol 173: 6000–6008.

115. Hemler ME (2001) Specific tetraspanin functions. J Cell Biol 155: 1103–1107.

116. Heijnen HF, Van Lier M, Waaijenborg S, Ohno-Iwashita Y, Waheed AA, Inomata M, Gorter G, Mobius W, Akkerman JW, Slot JW (2003) Concentration of rafts in platelet filopodia correlates with recruitment of c-Src and CD63 to these domains. J Thromb Haemost 1: 1161–1173.

117. Chirco R, Liu XW, Jung KK, Kim HR. Novel functions of TIMPs in cell signaling. Cancer & Metastasis Reviews 2006;25:99–113.

118. Holten-Andersen MN, Fenger C, Nielsen HJ, Rasmussen AS, Christensen IJ, Brunner N, Kronborg O. Plasma TIMP-1 in patients with colorectal adenomas: a prospective study. European Journal of Cancer 2004;40:2159–2164.

119. Fresno Vara JA, Casado E, de Castro J, et al. PI3K/Akt signalling pathway and cancer. Cancer Treat Rev 2004;30(2):193–204.

120. Sansal I, Sellers WR. The biology and clinical relevance of the PTEN tumor suppressor pathway. J Clin Oncol 2004;22(14):2954–63.

121. Karakas B, Bachman KE, Park BH. Mutation of the PIK3CA oncogene in human cancers. Br J Cancer 2006;94(4):455–9.

122. Garcia-Rostan G, Costa AM, Pereira-Castro I, et al. Mutation of the PIK3CA gene in anaplastic thyroid cancer. Cancer Res 2005;65(22):10199–207.

123. Ringel MD, Hayre N, Saito J, et al. Overexpression and overactivation of Akt in thyroid carcinoma. Cancer Res 2001;61(16):6105–11.

124. Hou P, Liu D, Shan Y, et al. Genetic alterations and their relationship in the phosphatidylinositol 3- kinase/Akt pathway in thyroid cancer. Clin Cancer Res 2007;13(4):1161–70.

125. Vasko V, Ferrand M, Di Cristofaro J, et al. Specific pattern of RAS oncogene mutations in follicular thyroid tumors. J Clin Endocrinol Metab 2003;88(6):2745–52.

126. Liu Z, Hou P, Ji M, Guan H, Studeman K, Jensen K, Vasko V, El-Naggar AK, Xing M. Highly prevalent genetic alterations in receptor tyrosine kinases and phosphatidylinositol 3-kinase/akt and mitogen-activated protein kinase pathways in anaplastic and follicular thyroid cancers. J Clin Endocrinol Metab. 2008 Aug;93(8):3106-16.

127. Kitchener P, Di Blasi F, Borrelli E, & Piazza PV. Differences between brain structures in nuclear translocation and DNA binding of the glucocorticoid receptor during stress and the circadian cycle. Eur J Neurosci 2004; 19: 1837-1846.

128. Hingorani SR, Jacobetz MA, Robertson GP, Herlyn M, Tuveson DA. Suppression of BRAF(V599E) in human melanoma abrogates transformation. Cancer Res 2003; 63: 5198-5202.

129. Mesa C, Mirza M, Mitsutake N, et al. Conditional activation of RET/PTC3 and BRAFV600E in thyroid cells is associated with gene expression profiles that predict a preferential role of BRAF in extra cellular matrix remodeling. Cancer Res 2006; 66: 6521-6529.

130. Liu D, Xing M. Potent inhibition of thyroid cancer cells by the MEK inhibitor PD0325901 and its potentiation by suppression of the PI3K and NF-κB pathways. Thyroid 2008; 18: 853-864.

131. Yeh MW, Rougier JP, Park JW, et al. Differentiated thyroid cancer cell invasion is regulated through epidermal growth factor receptor-dependent activation of matrix metalloproteinase (MMP)-2/gelatinase A. Endocr Relat Cancer 2006; 13: 1173-1183.

132. Sounni NE, Noel A. Membrane type-matrix metalloproteinases and tumor progression. Biochimie 2005; 87: 329-342.

133. Shinohara M, Chung YJ, Saji M, Ringel MD. AKT in thyroid tumorigenesis and progression. Endocrinology 2007; 148: 942-947.

134. Pizzolanti G, Russo L, Richiusa P, et al. Fine-needle aspiration molecular analysis for the diagnosis of papillary thyroid carcinoma through BRAF V600E mutation and RET/PTC rearrangement. Thyroid 2007; 17: 1109-111.

135. Vale T, Ngo TT, White MA, Lipsky PE. Raf-induced transformation requires an interleukin 1 autocrine loop. Cancer Res 2001; 61:602–607